CR-137967

Princeton University

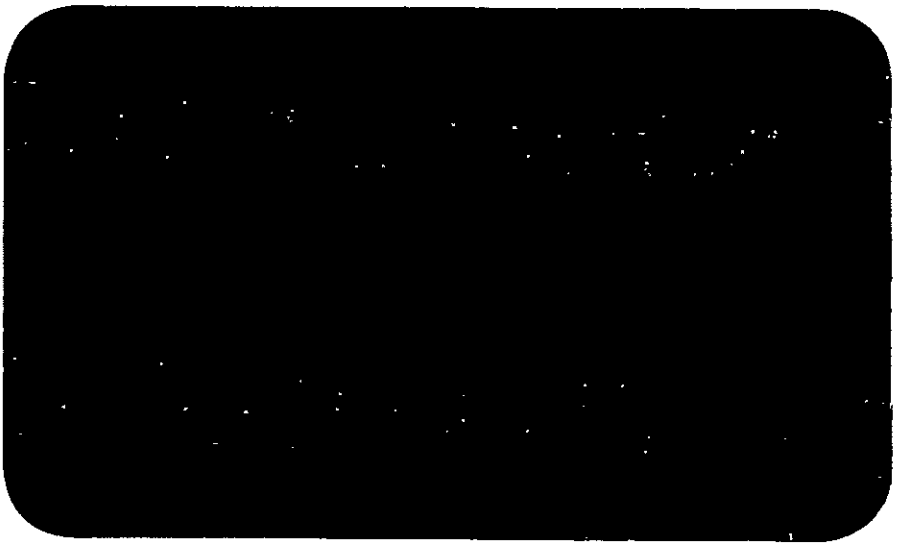

(NASA-CR-137967) SENSITIVITY OF HINGELESS ROTOR BLADE FLAP-LAG STABILITY IN HOVER TO ANALYTICAL MODELLING ASSUMPTIONS (Princeton Univ., N.J.) 99 p HC A05/MF A01 CSCL 01A

N77-10007

Unclas

G3/02 08055

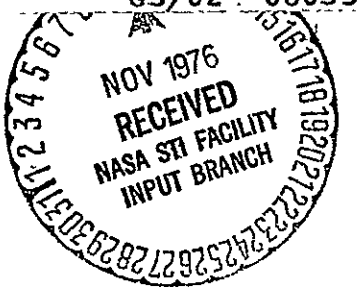

Department of
Aerospace and
Mechanical Sciences

CR-137967

SENSITIVITY OF HINGELESS ROTOR BLADE FLAP-LAG STABILITY IN HOVER TO ANALYTICAL MODELLING ASSUMPTIONS

by

H. C. Curtiss, Jr.

AMS Report No. 1236

January 1975

PREPARED UNDER

NASA-Ames Research Center
U. S. Army Air Mobility R&D Laboratory
Moffett Field, California

Contract Number NAS 2-7615

Princeton University
Department of Aerospace and Mechanical Sciences

FOREWORD

This technical report was prepared by the Department of Aerospace and Mechanical Sciences, Princeton University, Princeton, New Jersey under Contract Number NAS 2-7615 with NASA-Ames Research Center. It was funded by and under the technical direction of the U. S. Army Air Mobility Research and Development Laboratory, Ames Directorate, Ames Research Center at Moffett Field, California and was monitored and administered by Dr. Dewey H. Hodges of that directorate.

SUMMARY

This report considers some aspects of the prediction of flap-lag instabilities of hingeless rotor blades in hovering flight. Of particular interest is the sensitivity of analytical predictions of flap-lag stability to various analytical modelling assumptions. The dependence of the characteristic modes of motion on blade pitch angle is examined for various analytical models using root locus techniques.

Prediction of flap-lag stability using a single bending mode for each degree-of-freedom is examined in the case in which the bending modes are assumed to be the same in the flap and lag directions and are independent of pitch angle and stiffness distribution. It is shown that this model gives results analogous to those obtained by Ormiston employing a rigid blade model with the blade and hub stiffness represented by springs in the limiting cases of the elastic coupling parameter R = 0 and 1. For intermediate values of R the results are shown to be quite different. The mode shape assumptions are shown to result in what is referred to as the parallel spring model in contrast to Ormiston's model which is referred to as a series spring model. The similarities and differences between these two models is developed in some detail. The differences between these two models are examined for various typical rotor blade characteristics. Other aspects of the sensitivity of this problem are also considered.

The notation used and the basic development of the rigid blade equations follows that of two papers: "Linear Flap-Lag Dynamics of

Hingeless Helicopter Rotor Blades in Hover", by Ormiston and Hodges, Journal of the American Helicopter Society, April 1972, and "A Study of Stall-Induced Flap-Lag Instability of Hingeless Rotors", by Ormiston and Bousman, Journal of the American Helicopter Society, January 1975.

This report also indicates how equivalent lumped spring constants and masses are determined from a modal analyses of a rotor blade.

TABLE OF CONTENT

LIST OF FIGURES

LIST OF SYMBOLS

NOTE: Frequencies are non-dimensionalized by rotor RPM, Ω, time by $1/\Omega$, lengths by rotor radius, R, and velocities by $R\Omega$. Where the discussion in the text is self-contained in a specific section, additional definitions have been introduced to expedite the discussion which are not listed below.

a	linear two-dimensional section lift curve slope
A^{xwv}, A^{vw}, $A^{x\theta wv}$, A^{wv}, $A^{\theta vv}$, $A^{xx\theta w}$, A^{xw} and a^{xwv}, etc., $\tilde{a}^{xwv}$, etc.	see Appendix I
c	blade chord
C_{do}	profile drag coefficient at zero angle of attack
C_β, $C_{\dot\beta}$, C_ζ, $C_{\dot\zeta}$	see equations (1), (2), (3)
D	see equation (15) et. seq.
D_F, D_L	see equation (17) et. seq.
E	modulus of elasticity
F_β, $F_{\dot\beta}$, F_ζ, $F_{\dot\zeta}$	see equations (1), (2) and (3)
I_1	flapping moment of inertia of blade, $\int_o^R mr^2\,dr$
$I_{y'}$, $I_{z'}$	flap, lag bending area moments
$K^{vv\theta}$, $K^{ww\theta}$, $K^{vw\theta}$, K^{Vv}, K^{Vw}, $K^{V\dot v v}$, $K^{V\dot v w}$, and $k^{vv\theta}$, etc.	see Appendix I

L	see equation (2)
M^{xw}, $M^{uv\dot{v}v}$, $M^{uw\dot{w}v}$, $M^{\dot{w}v}$, M^{vv}, $M^{\dot{v}v}$, $M^{\dot{v}w}$, $M^{\ddot{w}w}$, and m^{xw}, etc.	see Appendix I
m	hub-blade mass per unit length
N	see equation (2)
p	(dimensionless) rotating flap natural frequency, $[1 + \omega_\beta{}^2]^{\frac{1}{2}}$
q	(dimensionless) rotating lag natural frequency, ω_ζ
R	elastic coupling parameter, see equation (23) et. seq. herein and equation (9) Reference 2; rotor blade radius
R_β, R_ζ	ratios of blade spring flexibility to combined spring flexibility for flap and lead-lag spring restraints, see equation (23) et. seq.
r	blade radial coordinate
r_h	radial position where blade-hub connect
s	(non-dimensional) Laplace transform variable
v	lead-lag deflection
v_i	induced velocity at 3/4 radius
w	flap deflection
x	r/R

β	blade flapping angle
Δ	see equation (2)
δ	see equation (6)
γ	$\rho a c R^4/I_1$ Lock Number
γ_p	principal axes rotation angle
ζ	blade lead-lag angle
η	$\gamma/8$
θ	blade pitch angle at 3/4 radius
ρ	air density
σ	real part of eigenvalue (pole or zero)
ϕ_i	$v_i/\Omega r$; $\phi_T = 4/3\ \phi_i$
ω	imaginary part of eigenvalue (pole or zero)
ω_ζ, ω_β	uncoupled lead-lag and flap mode non-rotating natural frequencies
ω_{ζ_B}, ω_{β_B}	natural frequencies of blade rigidly mounted (i.e., clamped at blade root)
Ω	rotor angular velocity, RPM or rad/sec
ψ_v, ψ_w	lag, flap elastic mode shapes
$(\ )_o$, $\Delta(\ )$	steady state and perturbation quantities
$[\ ]^T$	transpose of a matrix

INTRODUCTION

It has been shown[1] that hingeless rotor blades may experience instabilities owing to the coupling between out-of-plane (flap) bending and in-plane (lag) bending. The coupling between the flap motion and the lag motion arises from aerodynamic, elastic and inertial forces acting on the rotor blade.

The stability boundaries of this coupled motion appear to exhibit a considerable sensitivity to the approximations employed in developing the equations of motion. This is a result of the fact that the damping of the in-plane bending motion is very small in the uncoupled case and therefore, comparatively small coupling terms can destabilize the coupled motion.

This report examines some aspects of the sensitivity of flap-lag motion stability to various assumptions which may be employed.

Of particular interest here is the examination of various modelling assumptions associated with describing the structural properties of the blade/hub system.

In order to be able to conduct parametric studies of flap-lag stability, one particularly convenient approximation to the bending motion of the blades is to assume that only a single mode is required in each direction of bending and further that the mode shapes employed are those of a non rotating uniform cantilever beam.

Another approximate treatment has been suggested in the literature[1] which assumes that the blade and hub structural properties can be

represented by torsional springs located at the root of the blade. The blade is assumed to be rigid and the hub stiffness is represented by a set of springs which remain at a fixed orientation to the rotor shaft. The blade stiffness is represented by a set of springs which rotate as the blade pitch angle is changed. This lumped model is particularly convenient for obtaining insight into the manner in which various structural parameters enter into the stability analysis of flap-lag motion.

A basic parameter in the flap-lag stability problem is the blade pitch angle (or thrust level) of the rotor. Typically, instabilities occur as the blade pitch angle is increased[1]. The importance of the blade pitch angle to the instability, as well as the sensitivity of the analysis noted earlier, raises the question of whether the two approximate models described above result in a similar functional dependence of the structural properties (the stiffness matrix) of the blade/hub system on blade pitch angle.

Physically it would be expected that there would be a difference in these two models for the following reason. If it is assumed that the mode shapes of the hub/blade system are independent of the distribution of stiffness then as the stiffness is varied, the relative deflections between segments remain the same since the mode shape does not change. As a result, local equilibrium along the blade is not satisfied as stiffness is varied and the assumption of a fixed mode shape is equivalent to assuming

that various segments deflect proportional to each other independent of stiffness. This is in contrast to the model in which the hub stiffness is modelled as a pair of torsion springs and the blade stiffness is modelled as a pair of torsion springs. This model, taken with the assumption that the hub has no mass, determines a relative deflection between the hub and the blade which is a function of the relative stiffness of the hub spring and the blade spring. This spring model is referred to as a series spring model implying that relative deflection between the inner spring (hub) and the outer spring (blade) is determined by the relative spring stiffness.

It would be expected that the approach in which it is assumed that the mode shapes do not depend on stiffness would be analogous to the assumption that the relative deflections of the hub and blade are proportional and that the constant of proportionality does not depend on the relative stiffness of the hub and blade. This assumption corresponds to what is referred to as a parallel spring configuration in the following.

The similarities and differences between these two modelling approaches, the spring model of Reference 1 and the fixed mode shape model are developed in detail in this report. A spring model is developed which is equivalent to the fixed mode analysis in the sense that it produces an identical dependence of the stiffness matrix on blade pitch angle as the fixed mode analysis. The pitch dependence of this model, referred to as a parallel spring model, is compared to the pitch dependence obtained from the series

spring model and the differences discussed.

Also root locus techniques are developed to study the influence of various parameters on the stability of the flap-lag motion with particular reference to the importance of the difference in pitch angle dependence obtained from the two model assumptions.

ROOT LOCUS STUDY

Owing to the sensitivity of the problem of predicting flap-lag stability of a hingeless rotor blade, an examination of the problem employing root locus techniques is highly desirable. This technique can be conveniently used if it is assumed that the blade pitch angle is small. The following analysis considers, in particular, the sensitivity of the movement of the flap-lag roots with increasing blade pitch to various assumptions which may be empolyed in studying the problem. The difference between the results obtained if a flexible blade model is used in contrast to a rigid blade with springs at the root is considered. The influence of a simple approximation to the inflow is also examined. Further, the results obtained using a series spring model are contrasted with those obtained with a parallel spring model. It is shown elsewhere in this report that the parallel spring model is analogous to the results obtained from a flexible blade model in which the mode shapes are taken to be independent of pitch angle.

First the characteristic equation describing the flap-lag motion is developed in a form suitable for root locus studies.

The perturbation equations for the flap-lag motion given by Ormiston/Hodges/Bousman[1,2] are

$$\begin{bmatrix} s^2 + F_\beta^\bullet s + F_\beta & -sF_\zeta^\bullet + F_\zeta \\ -sC_\beta^\bullet + C_\beta & s^2 + C_\zeta^\bullet s + C_\zeta \end{bmatrix} \begin{Bmatrix} \Delta\beta \\ \Delta\zeta \end{Bmatrix} = 0 \qquad (1)$$

where

$$F_\beta \equiv 1 + \frac{1}{\Delta}\left[\omega_\beta^2 + N \sin^2\theta\right]$$

$$C_\zeta \equiv \frac{1}{\Delta}\left[\omega_\zeta^2 - N \sin^2\theta\right]$$

$$C_\beta = F_\zeta \equiv \frac{N}{2\Delta} \sin 2\theta$$

$$\Delta \equiv 1 + NL \sin^2 \theta \qquad (2)$$

where $N \equiv R(\omega_\zeta^2 - \omega_\beta^2)$

$$L \equiv (1-R)\left(\frac{\omega_\zeta^2 - \omega_\beta^2}{\omega_\zeta^2\ \omega_\beta^2}\right) = \frac{N}{\omega_\beta^2\ \omega_\zeta^2}\ \left(\frac{1-R}{R}\right)$$

R - as defined in Equation (9) of Reference 2; see Equation (23) et.seq. herein.

The notation N and L are introduced so that the matched stiffness case ($\omega_\beta^2 = \omega_\zeta^2$) can be conveniently discussed. In addition these definitions serve to distinguish between the series spring model as developed by Ormiston[1,2] and the parallel spring model as developed in a later section of this report. It is shown that the parallel spring model is equivalent to the formulation with $\Delta = 1$; i.e., setting $L = 0$ in the resulting characteristic equation gives the characteristic equation for the parallel spring model.

The remaining terms in the equations of motion are

$$F_\beta^\bullet \equiv \eta$$

$$F_\zeta^\bullet \equiv \eta\ (2\theta - \phi_i) - 2\beta_o \qquad (3)$$

$$C_\beta^\bullet \equiv -\eta\ (\theta - 2\phi_i) + 2\beta_o$$

$$C_\zeta^\bullet \equiv \eta\ \left(2\,\frac{C_{do}}{a} + \theta\phi_i\right)$$

where $\eta \equiv \frac{\gamma}{8}$ and structural damping has been neglected.

The coning angle is given by the steady state equations as

$$\begin{bmatrix} F_\beta & F_\zeta \\ C_\beta & C_\zeta \end{bmatrix} \begin{Bmatrix} \beta_o \\ \zeta_o \end{Bmatrix} = \eta \begin{Bmatrix} (\theta - \phi_i) \\ -\frac{C_{do}}{a} - \theta\phi_i + \frac{9}{8}\phi_i^2 \end{Bmatrix} \tag{4}$$

Therefore the coning angle β_o is equal to

$$\beta_o = \frac{\eta C_\zeta (\theta - \phi_i) - \eta F_\zeta \left[-\frac{C_{do}}{a} - \theta\phi_i + \frac{9}{8}\phi_i^2\right]}{F_\beta C_\zeta - C_\beta F_\zeta} \tag{5}$$

It is assumed that the pitch angle is small such that $\sin\theta \cong \theta$, $\cos\theta \cong 1$. Further, it is assumed that the inflow angle at three quarters radius, ϕ_i, can be approximated by the following expression

$$\phi_i \cong \delta\frac{\theta}{2} \tag{6}$$

noted in an earlier paper by Ormiston[1] with $\delta = 1$. The constant δ is retained to permit examination of this approximation. It can be seen in the paper by Ormiston[1] that for a solidity in the neighborhood of .15, $\delta = 1$ is quite a reasonable approximation; however, as the solidity is reduced, comparison of this result with momentum theory indicates that a smaller value of δ should be chosen to approximate inflow dependence on pitch angle. A δ of 0.5 will be examined to approximate the low solidity case.

Further, consistent with the approximation that the pitch angle is small, the following approximation is made

$$\frac{1}{\Delta} = \frac{1}{1 + NL\sin^2\theta} \cong 1 - NL\theta^2 \tag{7}$$

This is a consistent approximation when the pitch angle is assumed small, except possibly in the case of a high chordwise stiffness.

The form of the result for the characteristic equation is such that it is necessary only to retain the linear term for the dependence of coning angle on blade pitch to obtain the dependence of the flap-lag roots on pitch angle. Therefore, introducing the notation $p^2 = 1 + \omega_\beta^2$

$$\beta_o \cong \frac{\eta\theta}{p^2} \left(1 - \frac{\delta}{2}\right) \tag{8}$$

The small term depending on blade profile drag has been neglected.

The various terms in the equations of motion are therefore, approximately, using (8) in (2) and (3)

$$\begin{aligned}
F_\beta &\cong p^2 + N \left(1 - L\omega_\beta^2\right) \theta^2 \\
C_\zeta &\cong \omega_\zeta^2 - N \left(1 + L\omega_\zeta^2\right) \theta^2 \\
C_\beta &= F_\zeta \cong N \theta \\
F_{\dot\beta} &= \eta \\
F_{\dot\zeta} &= 2\eta\theta \left\{\left(1 - \frac{\delta}{4}\right) - \frac{1}{p^2}\left(1 - \frac{\delta}{2}\right)\right\} \\
C_{\dot\beta} &= 2\eta\theta \left\{\left(\frac{-1+\delta}{2}\right) + \frac{1}{p^2}\left(1 - \frac{\delta}{2}\right)\right\} \\
C_{\dot\zeta} &= \eta \left(2\frac{C_{do}}{a} + \frac{\delta}{2}\theta^2\right)
\end{aligned} \tag{9}$$

The characteristic equation is from (1)

$$\left(s^2 + F_{\dot\beta}s + F_\beta\right)\left(s^2 + C_{\dot\zeta}s + C_\zeta\right) - \left(sF_{\dot\zeta} - F_\zeta\right)\left(sC_{\dot\beta} - C_\beta\right) = 0 \tag{10}$$

Using the approximations from (9) and retaining only terms of order θ^2 for the pitch angle dependence, the following is obtained from (10)

$$(s^2 + \eta s + p^2)\left(s^2 + \eta\left(2\frac{C_{do}}{a}\right)s + \omega_\zeta^2\right)$$

$$+ \theta^2\left[\frac{\eta\delta}{2}s\left\{s^2 + \eta\left(1 + \frac{2}{\delta}\left(1 - \frac{\delta}{2}\right)^2\left(\frac{6p^2 - 4}{p^4}\right) + \frac{4}{\delta}\left(1 - \frac{\delta}{4}\right)(1 - \delta)\right)s\right.\right.$$

$$\left.\left. p^2\right\} + N\left(\eta\frac{\delta}{2}s + \frac{N(1-R)}{R} - 1\right)\right.$$

$$\left. -NL\omega_\zeta^2\left(\left(1 + \frac{\omega_\beta^2}{\omega_\zeta^2}\right)s^2 + \eta s + (1 + 2\omega_\beta^2)\right)\right] = 0 \qquad (11)$$

where the N, L notation has been retained at this point so that the parallel and series spring models may be clearly distinguished.

For the parallel spring model

$$L = 0 \qquad (12)$$

For the series spring model of Ormiston[1]

$$L = \frac{N}{\omega_\beta^2\,\omega_\zeta^2}\left[\frac{1 - R}{R}\right] \qquad (13)$$

The parameter $N = R(\omega_\zeta^2 - \omega_\beta^2)$ and was introduced to make it convenient to examine the matched stiffness case. For the flexible blade case, the characteristic equation will of course be of similar form with different coefficients as will be noted later.

The lag damping term ensuing from the profile drag of the blade $\left(\eta\frac{2C_{do}}{a}\right)$ has been neglected when it appears added to the flap damping η.

Now, consider various cases of interest in flap-lag stability. First it may be noted that in either of two particular values of the elastic coupling paramter R; R = 0 (the principal axes of the blade/hub system remain parallel and perpendicular to the rotor shaft and do not rotate with pitch) and R = 1 (the principal axes of the blade/hub system rotate an equal amount as the blade pitch angle), the parallel and series spring

models yield the same characteristic equation since L = 0 when R = 1 for the series spring model. These two limiting cases are considered first.

a.) No Elastic Coupling (R = 0)

In this case N = 0 and the characteristic equation reduces to

$$(s^2 + \eta s + p^2)\left(s^2 + \eta\left(2\frac{C_{do}}{a}\right)s + \omega_\zeta^2\right) + \frac{\eta\delta}{2}\theta^2\left[s\left\{s^2 + \eta\left(1 - \frac{2}{\delta}\left(1 - \frac{\delta}{2}\right)^2\left(\frac{6p^2 - 4}{p^4}\right) + \frac{4}{\delta}\left(1 - \frac{\delta}{4}\right)(1 - \delta)\right)s + p^2\right\}\right] = 0 \qquad (R = 0) \qquad (14)$$

The poles of this locus are the uncoupled flap and lag motion. There are three zeros, one at the origin, and a complex pair with imaginary parts approximately located at the uncoupled rotating flap frequency, and real parts dependent upon the uncoupled rotating flap frequency (p^2) and the assumption regarding inflow (the parameter δ) and the Lock number.

Select the following physical parameters

$$p^2 = 1.33$$

$$\eta = .625 \quad (\gamma = 5)$$

$$a = 5.73$$

$$C_{do} = .01$$

such that the results may be directly compared with Ormiston/Bousman.[2] The influence of various values of the lag frequency are of interest so it is not selected at this point. With these values (14) becomes

$$(s^2 + .625 + 1.333)(s^2 + .002\ s + \omega_\zeta^2)$$

$$+ .3125\,\delta\,\theta^2 \left[s \left\{ s^2 + .625 \left(1 - \frac{4.5}{\delta} \left(1 - \frac{\delta}{2}\right)^2 + \frac{4}{\delta}\left(1 - \frac{\delta}{4}\right)(1 - \delta) \right) s \right.\right.$$

$$\left.\left. + 1.333 \right\} \right] = 0 \qquad (15)$$

If $\delta = 1$, the quadratic factor for the zeros is equal to

$$[s^2 - .0785 + 1.333]$$

If $\delta = .5$, this quadratic factor is equal to

$$[s^2 - .352\, s^2 + 1.333]$$

Note the strong influence of the inflow model on the location of the real part of the complex zeros. Note also that the parameter δ appears in the root locus gain. Denote

$$D = \eta \frac{4}{\delta} \left(1 - \frac{\delta}{2}\right)^2 \quad \frac{(p^2 - 1)(p^2 - 2)}{p^4}$$

such that the characteristic equation is

$$(s^2 + .6255 + 1.333)(s^2 + .002\, s + \omega_\zeta^2)$$

$$+ .3125\,\delta\,\theta^2 \left[s\,(s^2 + Ds + 1.333) \right] = 0 \qquad (16)$$

As an aside, before discussing the root locus, a simple result can be obtained for the coupled roots in the special case where $\omega_\zeta^2 = p^2 = 1.333$. Neglecting the blade profile drag term, this case results in the characteristic equation of the form

$$(s^2 + D_f s + p^2)(s^2 + D_L s + p^2) = 0 \qquad (17)$$

where

$$\eta \left(1 + \frac{\delta\theta^2}{2}\right) = D_f + D_L$$

$$\eta \frac{\delta}{2} \theta^2 D = D_f D_L$$

and since the lag damping is small

$$D_f \cong \eta \left(1 + \frac{\delta\theta^2}{2} \right)$$
$$D_L \cong \frac{\delta}{2} D\theta^2 \qquad (18)$$

showing that a negative value of D leads to an instability in the lag motion. For the particular values above the lag damping as a function of pitch angle is given by

$$D_L \cong -.039\,\theta^2 \qquad (\delta = 1)$$
$$D_L \cong -.088\,\theta^2 \qquad (\delta = .5)$$

in the special case where $\omega_\zeta^2 = p^2$. Note the sensitivity of the result to the selection of the inflow parameter δ.

Now to continue with the root locus considerations. Figure 1 shows the location of the zeros and poles for $\omega_\zeta = 1.1$ and the locus of lag roots. The lower figure with $\delta = 0.5$, corresponding to a low solidity agrees well with Figure 6 of Ormiston[1], et. al., as would be expected. For simplicity the flap mode trend is not shown. The form of this locus will be quite similar for other cases since the complex zeros are located at the flap frequency. It can be clearly seen that the most critical case as far as destabilizing the flap mode is concerned occurs when ω_ζ^2 is in the vicinity of p^2. Figure 2 shows the influence of lag frequency on the locus. δ is taken as 0.5 to agree with Ormiston's results presented in Figure 6 of his paper.[1]

Note particularly the importance of the inflow approximation (or essentially solidity); a value of $\delta = 1.0$ indicates that small pitch angles will stabilize the lag mode for $\omega_\zeta = 1.4$ where a $\delta = 0.5$ indicates that increasing pitch angle destabilizes the lag mode. At $\omega_\zeta = .7$ the trend is less sensitive to δ. The matched stiffness case presents a special situation discussed later.

Recall that there is no influence of the parallel or series spring approximation.

b.) Full Elastic Coupling (R = 1)

Now consider the other limit in which R = 1. The characteristic equation in this case is from (11), recalling the definition of D,

$$(s^2 + \eta\, s + p^2)\left(s^2 + \eta\, \frac{2C_{do}}{a}\, s + \omega_\zeta^2\right)$$

$$+ \theta^2\left[\frac{\eta\delta}{2}\, s\,(s^2 + D s + p^2) + (\omega_\zeta^2 - \omega_\beta^2)\left(\eta\, \frac{\delta}{2}\, s - 1\right)\right] = 0 \qquad (19)$$

The zero location for the root locus now depends upon the difference between the nonrotating flap and lag frequencies. A locus of zeros with variation in ω_ζ can be conveniently sketched as shown in Figure 3. The matched stiffness case is the same zero location as R = 0 for the special case when $R_\beta = R_\zeta$, and this locus is the same for either the series or parallel spring model. The matched stiffness case is treated in detail later. There is a difference between the parallel spring model and the series spring model when $R_\beta \neq R_\zeta$.

With the zero locations given, the root locus for increasing pitch angle for various values of lag frequency can be conveniently sketched as shown in Figure 4. Generally in this case where R = 1, the lag mode is stabilized by increasing pitch angle. At higher lag frequencies there appears to be a tendency towards instability but care must be taken with the approximations as noted.

These two limiting cases of R = 0 and R = 1 serve as a valuable view of the limits encountered in the more general case of values of R between zero and one. The zeros of the loci for increasing pitch angle at various

intermediate values of R will move from the location shown in Figure 1 to the location shown in Figure 3. However, it should also be recalled that in the cases where a value of R between zero and one is considered there will be a difference between the results depending upon whether the parallel spring model or the series spring model is employed. Recall also that the parallel spring model is analogous to a flexible blade model with an assumption of mode shapes independent of pitch.

c.) Intermediate Elastic Coupling ($0<R<1$).

In this case the characteristic equation will differ in the parallel spring case ($L = 0$) from the series spring case

$$L = \frac{N}{\omega_\beta^2 \, \omega_\zeta^2} \left(\frac{1 - R}{R}\right)$$

The characteristic equation for the parallel spring model is from (11)

$$(s^2 + \eta\, s + p^2)\left(s^2 + \eta \left(\frac{2C_{do}}{a}\right) s + \omega_\zeta^2\right)$$

$$+ \frac{\eta\delta}{2}\theta^2 \left[s\,(s^2 + Ds + p^2) \right.$$

$$\left. + R\,(\omega_\zeta^2 - \omega_\beta^2)\left(s + \frac{2}{\eta\delta}\left[(\omega_\zeta^2 - \omega_\beta^2)(1 - R) - 1\right]\right)\right] = 0 \qquad (20)$$

Note that the zero location bears a certain similarity to the $R = 1$ case with the exception of the term

$$\frac{2}{\eta\delta}(\omega_\zeta^2 - \omega_\beta^2)(1 - R)$$

Without this term, the locus of zeros with R varying would be identical to the locus shown in Figure 3 for ω_ζ varying with $R = 1$.

For the series spring model, the characteristic equation is

$$(s^2 + \eta s + p^2)\left(s^2 + \eta\left(2\frac{C_{do}}{a}\right) s + \omega_\zeta^2\right)$$

$$+ \theta^2 \left[\frac{\eta\delta}{2} s (s^2 + Ds + p^2) \right.$$

$$+ R(\omega_\zeta^2 - \omega_\beta^2) \left\{ \frac{\eta\delta}{2} s + (\omega_\zeta^2 - \omega_\beta^2)(1 - R) - 1 \right\}$$

$$\left. - (1 - R)\left(\frac{\omega_\zeta^2}{\omega_\beta^2} - 1\right) \left(\left(1 + \frac{\omega_\beta^2}{\omega_\zeta^2}\right) s^2 + \eta s + (1 + 2\omega_\beta^2) \right) \right] = 0 \qquad (21)$$

where there is an additional quadratic factor in the expression for the zeros, the underlined terms, which arise in the series spring model, but are not present in the parallel spring model.

The series spring model will yield results which are the same as those obtained by Ormiston and shown in Figure 6 of his paper.[1] The parallel spring model will yield quite different results.

First consider the case in which the lag frequency $\omega_\zeta = 1.1$. Substituting this and the other values

$p^2 = 1.333$	$a = 5.73$	$D = -.078$	$\delta = 1$
$\eta = .625$	$C_{do} = 0.01$	$D = -.352$	$\delta = .5$

the characteristic equation becomes

$$(s^2 + .6255 + 1.333)(s^2 + .002 s + 1.21)$$

$$+ .3125 \delta \theta^2 \left[s (s^2 + D s + 1.333) \right.$$

$$+ .88R \left(s + \frac{3.2}{\delta} (.88(1 - R) - 1) \right)$$

$$\left. -(1 - R)\left(\frac{8.416}{\delta}\right)(1.275 s^2 + .625 s + 1.666) \right] = 0$$

where the underlined terms are dropped for the parallel spring model. In this example we select $\delta = 1$, giving the following characteristic equation

$$(s^2 + .625\,s + 1.333)\,(s^2 + .002\,s + 1.21)$$
$$+ .3125\,\theta^2 \Big[(s)\,(s^2 - .078\,s + 1.333)$$
$$+ .88R \left\{ s + 3.2\,(.88(1 - R) - 1) \right\}$$
$$- 10.73\,(1 - R)\,(s^2 + .490\,s + 1.306) \Big] = 0$$

Now then to compare the series and parallel models the zero locations for the series and parallel cases are shown in Figure 5. For reference, the locus of zeros given in Figure 3 (R = 1) is included as this represents the limiting points.

Note the sensitivity of the zero locations to the use of the series or parallel model.

Figure 6 shows the equivalent diagram for $\omega_\zeta = 1.4$ where the characteristic equation is for $\delta = 1$,

$$(s^2 + .625\,s + 1.333)\,(s^2 + .002\,s + 1.21)$$
$$+ .3125\,\theta^2 \Big[(s)\,(s^2 - .078\,s + 1.333)$$
$$+ 1.63\,R \left\{ s + 3.2\,(1.63\,(1 - R) - 1) \right\}$$
$$- 18.43\,(1 - R)\,(s^2 + .535\,s + 1.426) \Big] = 0$$

Figure 6 shows the locus of zeros for $\omega_\zeta = 1.4$. It can again be seen that the zero location is quite sensitive to the model employed. Figure 7 then shows the difference in the departure angles for these two models for $\omega_\zeta = 1.1$ and $\omega_\zeta = 1.4$. The limiting cases (R = 0, R = 1) are the same,

however, the departure angles differ markedly again indicating the sensitivity of the dependence of the lag modes to modelling assumptions. Recall also that particularly at $\omega_\zeta = 1.4$, there is a sensitivity to the inflow parameter δ.

The parallel spring model also indicates one interesting special case, corresponding to a particular value of R, in which the locus configuration is similar to the R = 0 case. Note that this result will not agree with the series case. The particular value of R is

$$(\omega_\zeta^2 - \omega_\beta^2)(1 - R) = 1$$

or

$$R = 1 - \frac{1}{\omega_\zeta^2 - \omega_\beta^2}$$

For this specific value of R, the parallel spring model gives zeros at

$$s\,(s^2 + D\,s + \omega_\zeta^2) = 0$$

Thus this special case will always give a locus which is similar in shape to that obtained for R = 0. The complex zeros are located at the lag frequency and in the right half plane if D is negative.

d.) Matched Stiffness $(\omega_\zeta^2 = \omega_\beta^2)$

In the matched stiffness case the parameter N, introduced earlier is employed, rather than R which becomes infinite except in the case $R_\zeta = R_\beta$. Therefore

$$N = R(\omega_\zeta^2 - \omega_\beta^2) = \omega^2 \{R_\beta - R_\zeta\}$$

If $R_\beta = R_\zeta$, N = 0 and the matched stiffness case will be the same as R = 0.

If $R_\beta \neq R_\zeta$ as would be more typical of the rotor blade, then there will be a difference in the locus from the R = 0 case. The characteristic equation in this case is $\omega_\zeta^2 = \omega_\beta^2 = \omega^2$

$$(s^2 + \eta s + p^2)\left(s^2 + \eta\left(2\frac{C_{do}}{a}\right)s + \omega^2\right)$$

$$+ \theta^2\left[\frac{\eta\delta}{2}s\,(s^2 + Ds + p^2) + N\left(\frac{\eta\delta}{2}s - (N+1)\right)\right.$$

$$\left.\underline{+ \frac{2N}{\omega^2}\left(s^2 + \frac{\eta}{2}s + \frac{1 + 2\omega^2}{2}\right)}\right] = 0$$

where again the underlined terms appear in the series spring model and not in the parallel model.

Since in this case

$$N = \omega^4\left(\frac{1}{\omega_{\beta_B}^2} - \frac{1}{\omega_{\zeta_B}^2}\right) = \omega^2\,\Delta R \;;\quad \Delta R = R_\beta - R_\zeta$$

and a typical rotor blade would have a considerably higher chordwise frequency than flapwise, positive values of N are of interest.

The departure angles are shown in Figure 8 for the matched stiffness case again using the previous parameters

$\gamma = 5$ $\qquad$ $C_{Do} = .01$

$\omega^2 = .333$ $\qquad$ $a = 5.73$

for N = 0, where the blade stiffness is matched and the results are the same as for R = 0, and for $\Delta R = .75$ which would be more typical of a rotor blade.

The coupling in this case has a strong stabilizing tendency on the flap-lag motion. Again the two models exhibit a difference. ΔR could

be somewhat larger than shown. It is equal to (in terms of frequency)

$$\Delta R = \frac{\omega^2}{\omega_{\beta_B}^2}\left(1 - \frac{\omega_{\beta_B}^2}{\omega_{\zeta_B}^2}\right)$$

and so is essentially limited to a maximum value of about one. Negative values of ΔR would be highly unlikely physcially as this would imply that $\omega_{\beta_B} > \omega_{\zeta_B}$.

This completes the discussion of the rigid blade models and the comparison of the series and parallel spring models. Now the rigid and the flexible blade models will be compared. The flexible blade model considered here (See Appendix I for a discussion of the flexible blade equations of motion.) assumes that the mode shapes are independent of the blade/hub mass and stiffness distribution and as shall be seen is structurally equivalent to the parallel spring model discussed above.

If the flexible blade model is used to determine the stiffness terms in the equations of motion and consequently the equivalent terms in the rigid blade model, then these terms for the flexible blade model will be identical to those of the parallel spring model.

The differences in the equations of motion in the flexible blade case as compared to the rigid blade case, will arise therefore in the aerodynamic terms and the coning angle. The coefficients of these terms will be changed from the rigid blade values depending upon the mode shape employed.

In terms of the previous discussion the following terms in the characteristic equation are unchanged therefore,

$$F_\beta = p^2 + N \sin^2 \theta$$

$$C_\zeta = q^2 - N \sin^2 \theta$$

$$F_\zeta = C_\beta = \frac{N}{2} \sin 2\theta$$

where Δ is taken as 1 since mode shapes independent of pitch angle are employed. p^2 and q^2 are the rotating flap and lag frequencies and include the Southwell coefficient which no longer equals 1 as it does in the rigid blade case.

The remaining terms are as follows. A uniform mass blade is considered.

RIGID BLADE	FLEXIBLE BLADE
$F_\beta^{\cdot} = \eta$	$\eta\, \tilde{a}^{xwv}$
$F_\zeta^{\cdot} = \eta\,(2\theta - \phi_i) - 2\beta_o$	$F_\zeta^{\cdot} = \eta\,(\lambda\, \tilde{a}^{vw} + 2\,\tilde{a}^{x\theta vw}) - C_o\, \bar{w}^o$
$C_\beta^{\cdot} = -\eta\,(\theta - 2\phi_i) + 2\beta_o$	$C_\beta^{\cdot} = -\eta\,(\tilde{a}^{x\theta wv} + 2\lambda\, \tilde{a}^{wv}) + C_o\, \bar{w}^o$
$C_\zeta^{\cdot} = \eta\,(2\frac{C_{do}}{a}) + \theta\,\phi_i$	$C_\zeta^{\cdot} = \eta\,(2\frac{C_{do}}{a}\,\tilde{a}^{xwv} - \lambda\,\tilde{a}^{\theta vv})$

Table I gives the values of the various mode shape parameters given above when a Duncan polynomial is used for the first mode shape.

Substituting numerical values for an untwisted rotor blade the following results are obtained. The terms for the rigid blade can be obtained directly from the mode shape integrals with $\psi = x$. See Appendix I.

RIGID BLADE	FLEXIBLE BLADE
$F_\beta^{\cdot} = \eta$	$1.070\,\eta$
$F_\zeta^{\cdot} = \eta\,(2\theta - \phi_i) - 2\beta_o$	$\eta\,[2.140\theta - 1.335\,\phi_T] - 2.110\,\bar{w}^o$
$C_\beta^{\cdot} = -\eta\,(\theta - 2\phi_i) + 2\beta_o$	$-\eta\,[1.070\,\theta_o - 2.670\,\phi_T] + 2.110\,\bar{w}^o$
$C_\zeta^{\cdot} = \eta\,[2\frac{C_{do}}{a} + \theta\phi_i]$	$\eta\,[(1.070)\,(2\frac{C_{do}}{a}) + 1.335\,\theta\phi_T]$

The coning angle is given by

$$\beta_o = \frac{\eta}{p^2}(\theta - \phi_i) \qquad \bar{\bar{w}}^o_o = \frac{\eta}{p^2}(\tilde{\tilde{a}}^{xx\theta w} + \lambda\, \tilde{\tilde{a}}^{xw})$$

$$\beta_o = \frac{\eta}{p^2}(\theta - \phi_i) \qquad \bar{\bar{w}}^o = \frac{\eta}{p^2}[1.1688\,\theta - 1.5014\,\phi_T]$$

where $\phi_T = \frac{4}{3}\phi_i$ in the flexible blade equations, giving for the flexible blade the following coefficients

$$F_\beta = 1.070\,\eta$$

$$F^*_\zeta = \eta\,[2.140\,\theta - 1.001\,\phi_i] - 2.110\,\bar{\bar{w}}^o$$

$$C^*_\beta = -\eta\,[1.070\,\theta - 2.003\,\phi_i] + 2.110\,\bar{\bar{w}}^o$$

$$C^*_\zeta = \eta\,[1.070\,(2\,\frac{C_{do}}{a}) + 1.001\,\theta\,\phi_i]$$

$$\bar{\bar{w}}^o = \frac{\eta}{p^2}[1.1688\,\theta - 1.126\,\phi_i]$$

Introducing the approximation that $\phi_i = \frac{\theta}{2}$ where here for simplicity the $\delta = 1$ only case is examined.

$$F^*_\zeta = (1.640 - \frac{1.278}{p^2})\,\eta\theta$$

$$C^*_\beta = (-.068 + \frac{1.278}{p^2})\,\eta\theta$$

$$F^*_\beta = 1.070\,\eta$$

$$C^*_\zeta = \eta\,[1.070\,(2\,\frac{C_{do}}{a}) + .500\,\theta^2]$$

$$\bar{\bar{w}}^o = \frac{.6058\,\eta\theta}{p^2}$$

For comparison purposes, the rigid blade terms are

$$F_{\dot{\beta}} \doteq \eta$$

$$C_{\dot{\zeta}} = \eta \left[2 \frac{C_{do}}{a} + .5\,\theta^2\right]$$

$$F_{\dot{\zeta}} = \eta\,\vartheta \left(1.5 - \frac{1}{p^2}\right)$$

$$C_{\dot{\beta}} = \eta\,\theta \left(\frac{1}{p^2}\right)$$

$$\beta_o = \frac{.5\eta\,\theta}{p^2}$$

The significant change appears through the coning angle affecting primarily the coupling terms $F_{\dot{\zeta}}$ and $C_{\dot{\beta}}$.

$$(s^2 + F_{\dot{\beta}} s + F_\beta)(s^2 + C_{\dot{\zeta}} s + C_\zeta) - (C_{\dot{\beta}} s + C_\beta)(F_{\dot{\zeta}} s - F_\zeta) = 0 \qquad (10)$$

The R = 0 case will be examined for these two models when R = 0, $F_\zeta = C_\beta = 0$ and the pitch dependence appears in the $C_{\dot{\zeta}}$ term, the lag damping, and the coupling term $-C_{\dot{\beta}} F_{\dot{\zeta}} s^2$.

The characteristic equation is therefore, with the θ dependent terms separated out equal to

$$(s^2 + F_{\dot{\beta}} s + F_\beta)\left(s^2 + \eta \left(2 \frac{C_{do}}{a}\right) s + C_\zeta\right)$$

$$+ \theta^2 \frac{\eta}{2} s \left(s^2 + \left[F_{\dot{\beta}} - \frac{F_{\dot{\beta}} C_{\dot{\zeta}}}{\theta^2 \frac{\eta}{2}}\right] s + F_\beta\right) = 0 \qquad (22)$$

The term which determines the real part of the complex zeros is essentially the only place in which the difference in the two models appears. This is the term which was denoted as D earlier.

$$D = F_{\dot{\beta}} - \frac{F_{\dot{\beta}} C_{\zeta}}{\theta^2 \frac{\eta}{2}}$$

For the rigid blade model

$$D = \eta - \frac{2\eta}{p^2}\left(1.5 - \frac{1}{p^2}\right) = \eta \frac{(p^2 - 1)(p^2 - 2)}{p^4}$$

This shows clearly the limits in flap frequency found by Ormiston.[1] If $1 < p^2 < 2$ then the complex zeros for the pitch angle locus are located in the right half plane and for rotating lag frequencies in the vicinity of the flap frequency, the lag poles will be attracted to the right half plane by these complex zeros leading to instability with increasing pitch angle.

For the flexible blade (with Duncan polynomials for mode shapes)

$$D = 1.070\,\eta - 2\eta\left(1.640 - \frac{1.278}{p^2}\right)\left(\frac{1.278}{p^2} - .068\right)$$

$$D = 1.293\,\eta\ \frac{(p^2 - 2.257)(p^2 - 1.119)}{p^4}$$

Thus the flexible blade model with Duncan polynomials as mode shapes will give a somewhat different frequency range for instability. Instability would be expected for $1.12 < p^2 < 2.26$.

The location of the complex zeros as a function of p for the rigid and flexible models is shown in Figure 9.

The inflow model will affect these results. If $\delta = 0.5$ then the rigid blade model gives for D

$$D = 4.5\,\eta\ \frac{(p^2 - 1)(p^2 - 2)}{p^4}$$

It is interesting to note that selecting $\delta = 0.5$ does not change the range of flap frequency over which an instability would be expected but it does increase the movement of the complex zeros into the right half plane.

In the flexible blade case with $\delta = 0.5$,

$$D = 5.269\,\eta\,\frac{(p^2 - 2.35)(p^2 - 1.14)}{p^4}$$

There is again an increase in the variation of the real part of the complex zeros with changes in flap frequency and the frequency range over which the complex zeros are located in the right half plane is about the same as in the case where $\delta = 1$. Recall that δ also appears in the root locus gain so that these changes in the zero locations do not directly imply a proportional decrease in the stability of the lag mode.

In the particular case here note that for flap frequencies less than $\sqrt{1.12}$, in the case where $\delta = 1$, the flexible blade model will not predict an instability with increasing pitch angle while the rigid blade model will owing to the fact that the zeros for the flexible blade will be located in the left half plane.

Thus the nature of the stability of this system appears particularly sensitive to modelling assumptions for the elastically uncoupled case and the results will depend upon the assumptions employed. Physically this can be seen to arise from the fact that the real part of the complex zeros is located by a term which is the difference of the product of the flap damping and the part of the lag damping dependent upon pitch and

the rate coupling terms arising from aerodynamics and coriolus terms, i.e.,

$$\frac{1}{\theta^2}\left[\left(C_{\dot{\zeta}} - 2\frac{C_{do}}{a}\eta\right)F_{\dot{\beta}} - F_{\dot{\zeta}}C_{\dot{\beta}}\right]$$

The second term $F_{\dot{\zeta}}C_{\dot{\beta}}$ subtracts from the first and so this term may be of either sign and is quite sensitive to the assumptions employed in studying flap-lag stability. This is particularly the case when the uncoupled lag frequency is in the vicinity of the flap frequency such that the lag roots are directly attracted to these zeros. The important role played by the dependence of the lag damping on blade pitch can also be noted from this expression. If δ is set equal to zero, the lag damping becomes independent of pitch angle and there are two zeros at the origin. The root locus angle condition will be 0° for $1 < p^2 < 2$ and 180° for p^2 outside this range, indicating a more severe instability with increasing pitch in the range of $1 < p^2 < 2$. The presence of the lag damping dependence on pitch acts to limit the instability with increasing pitch to some maximum unstable damping as shown by the zero locations in Figure 9.

It is expected that the R = 1 case is not so sensitive as the zeros in this case are moved into the left hand plane by the additional structural terms introduced by elastic coupling as can be seen from Figure 3.

For small values of R it would be expected that the sensitivity to modelling assumptions will exist. It has already been shown that for small values of R, considerable differences exist between the use of a parallel spring model, corresponding to a fixed mode shape assumption and the series spring model proposed by Ormiston which physically appears to correspond to a more refined assumption regarding the variation of the mode shapes with blade pitch.

To summarize this discussion it can be seen that for a hingeless rotor blade with no elastic coupling the results of a flap-lag stability investigation are sensitive to the details of the assumptions made in the physical model.

For small values of the elastic coupling parameter a similar sensitivity exists which depends upon the nature of the structural model as well as the assumption regarding the inflow.

The fully elastically coupled blade (R = 1) does not appear to be particularly sensitive to modelling assumptions on the basis of these investigations and the same results are obtained from either the series spring model or the parallel spring model.

Intermediate values of R appear to give rise to a situation in which the results of a stability investigation are very sensitive to the modelling assumptions. There appears to be less sensitivity for blades which are soft in the chordwise direction than for blades which are stiff in the chordwise direction judging by comparison of the trends shown for a matched stiffness blade compared to the stiff inplane case. As the chordwise frequency is increased there appears to be an increasing sensitivity to the use of a series spring model as compared to the parallel spring model as can be seen by comparing Figures 5 and 6, implying that for intermediate values of R, the details of the modal analysis for a flexible blade are significant.

The root locus technique appears quite valuable in pointing out some of the sensitivities involved in this problem. It would be expected from these results that while the general shape of a stability diagram such as

shown in Figure 4 of Ormiston's paper[1] illustrates the nature of the stability boundaries for flap-lag stability, the precise values will be sensitive to the details of the model. Further it would appear that for the results shown in Figure 6 of Ormiston's paper, the trends shown for $0 < R < 0.4$ are also very sensitive to the particular analytical model used.

To make this point more concretely, Figures 10 - 12 have been prepared to show the locus of roots of the lag mode as a function of blade pitch for three values of the uncoupled lag frequency, based on the parallel spring model. These figures correspond to the root locus sketches in Figures 7 and 8. The figures may be directly compared with Figure 6 of the paper by Ormiston and Hodges[1] and illustrate the differences between the parallel spring model and the series spring model.

The two models give quite similar results for $\omega_\zeta = 0.7$ and considerably different results for $\omega_\zeta = 1.1$ and 1.4. Note the decreased sensitivity to pitch angle predicted by the parallel spring model as compared to the series spring model by Ormiston and Hodges.

THE PARAMETER R

The parameter R was introduced by Ormiston[1] to represent the elastic coupling of the blade/hub system. It can be conveniently interpreted as being directly related to the rotation of the principal axes of the blade/hub system. It can be shown that the rotation of the principal axes of the blade/hub system γ_p is related to the blade pitch angle and the parameter R by the following equation (see pp. 30 and 41)

$$\tan 2\gamma_p = \frac{R \sin 2\theta}{R \cos 2\theta + (1 - R)} \tag{23}$$

For small pitch anges this reduces approximately to

$$\gamma_p \cong R\,\theta$$

Figure 13 shows a graph of the principal axis inclination as a function of blade pitch angle for various values of R. Note that when R = 1, $\gamma_p = \theta$ for all values of θ, and when R = .5, $\gamma_p = \frac{\theta}{2}$.

In this investigation the range of R examined was between 0 and 1. By placing R in a somewhat different form, an estimate of the possible range of R can be seen. As defined by Ormiston[1]

$$R \equiv \frac{\omega_\zeta^2 R_\beta - \omega_\beta^2 R_\zeta}{\omega_\zeta^2 - \omega_\beta^2}$$

where

$$R_\beta \equiv \frac{\omega_\beta^2}{\omega_{\beta_B}^2}$$

$$R_\zeta \equiv \frac{\omega_\zeta^2}{\omega_{\zeta_B}^2}$$

where $\omega_{\beta_B}^2$ and $\omega_{\zeta_B}^2$ are the natural frequencies of the blade rigidly mounted. R can be expressed as

$$R = \left(\frac{1 - \frac{\omega_{\beta_B}^2}{\omega_{\zeta_B}^2}}{1 - \frac{\omega_\beta^2}{\omega_\zeta^2}} \right) \left(\frac{\omega_\beta^2}{\omega_{\beta_B}^2} \right)$$

It can be seen that R = 1 if the hub mounting has no influence on the natural frequencies such that

$$\omega_{\zeta_B} = \omega_\zeta$$

$$\omega_{\beta_B} = \omega_\beta$$

R = 0 if the blade itself is of matched stiffness, which is a physically unlikely situation unless the blade is softened at the root in the chordwise direction outboard of the pitch change bearing. R is also equal to zero if the blade is articulated in the flapwise direction such that $\omega_\beta = 0$. Thus in the root locus studies described in another section, the case R = 0 implies that outboard of the blade pitch bearing, the nonrotating frequencies in flap and lag are equal.

The case R = 1 can be achieved by a number of combinations including the situation in which the hub is very stiff such that the blade/hub frequencies are the same as the blade rigidly mounted. If the blade is not softened outboard of the pitch bearing then it would be expected that $\omega_{\beta_B}/\omega_{\zeta_B}$ would be small leading to a value of R which depends upon the blade/hub system frequency ratios and the reduction in the flapwise frequency ratio produced by the hub. This gives the possibility of R values larger than 1 particularly

for a blade/hub system which is soft in the chordwise direction.

Negative values of R, although theoretically possible from the form of the expression, appear to be highly unlikely in practice.

COMPARISON OF VARIOUS STIFFNESS MODELS

In this section, the form of the stiffness terms in the elastic blade equations are examined for the case in which it is assumed that the bending of the blade in the flap and lag directions is represented by a single mode and also that the mode shape is independent of the stiffness distribution between the blade and the hub. Of particular interest is functional dependence of the terms in the stiffness matrix on blade pitch angle. In addition two other simple models of the blade/hub system are examined. The hub and blade are modelled as rigid members with the hub stiffness represented by a spring at the root and the blade stiffness by a spring between the hub and the blade. Two alternate assumptions examined: one in which the blade deflection is assumed to be proportional to the hub deflection and independent of stiffness of the spring, and the second in which the relative deflection between the blade and the hub is determined from the condition of equilibrium of the hub segment[1]. These two models are referred to as the series spring model and the parallel spring model as well will be explained. The blade pitch dependence of the stiffness matrix for these two models is examined. It is shown that the parallel spring model yields a pitch dependence of the stiffness matrix identical to the modal analysis with fixed mode shapes and the series spring model yields different results, in general, as to the manner in which the stiffness matrix varies with blade pitch.

First consider the elastic stiffness terms as given by the flexible

blade equations of motion presented in Appendix I. The terms of interest here are:

$$\begin{bmatrix} K^{vv\theta} & K^{vw\theta} \\ K^{vw\theta} & K^{ww\theta} \end{bmatrix} \begin{Bmatrix} v \\ w \end{Bmatrix}$$

where

$$K^{vv\theta} = \int_o^R EI_{z'}(\psi_v'')^2 \, dr + \int_o^R (EI_{y'} - EI_{z'}) \sin^2\theta \, (\psi_v'')^2 \, dr$$

$$K^{ww\theta} = \int_o^R EI_{y'}(\psi_w'')^2 \, dr + \int_o^R (EI_{z'} - EI_{y'}) \sin^2\theta \, (\psi_w'')^2 \, dr$$

$$K^{vw\theta} = \int_o^R [EI_{z'} - EI_{y'}] \frac{\sin 2\theta}{2} (\psi_v'' \, \psi_w'') \, dr \qquad (24)$$

Now, if it is assumed that the mode shapes are independent of blade pitch, that is, they are the mode shapes calculated at zero pitch then the functional form of these stiffness coefficients is as follows

$$K^{vv\theta} = \int_o^R EI_{z'} (\psi_v'')^2 \, dr - \sin^2\theta \int_o^R (EI_{z'} - EI_{y'}) (\psi_v'')^2 \, dr$$

$$K^{ww\theta} = \int_o^R EI_{y'}(\psi_w'')^2 \, dr + \sin^2\theta \int_o^R (EI_{z'} - EI_{y'}) (\psi_w'')^2 \, dr$$

$$K^{vw\theta} = \sin\theta \cos\theta \int_o^R (EI_{z'} - EI_{y'}) (\psi_v'' \, \psi_w'') \, dr$$

If the rotor blade of interest is considered to consist of two portions, an inner segment denoted by the subscript h which does not rotate, extending to a radius r_h and an outer portion denoted by the subscript b which rotates with the pitch angle θ, the terms are

$$K^{vv\theta} = \int_o^{r_h} EI_{z'h} (\psi_v'')^2 \, dr + \int_{r_h}^{R} EI_{z'b} (\psi_v'')^2 \, dr -$$

$$- \sin^2 \theta \int_{r_h}^{R} (EI_{z'b} - EI_{y'b}) (\psi_v'')^2 \, dr$$

$$K^{ww\theta} = \int_o^{r_h} EI_{y'h} (\psi_w'')^2 \, dr + \int_{r_h}^{R} EI_{y'b} (\psi_w'')^2 \, dr$$

$$+ \sin^2 \theta \int_{r_h}^{R} (EI_{z'b} - EI_{y'b}) (\psi_w'')^2 \, dr$$

$$K^{vw\theta} = \sin \theta \cos \theta \int_{r_h}^{R} (EI_{z'b} - EI_{y'b}) (\psi_v'' \, \psi_w'') \, dr \qquad (25)$$

If it is further assumed that the mode shapes are the same for both directions of bending such that

$$\psi = \psi_v = \psi_w$$

and using the following notation

$$k_{zh} \equiv \int_o^{r_h} EI_{z'h} (\psi'')^2 \, dr$$

These coefficient become

$$K^{vv\theta} = k_{zh} + k_{zb} - \sin^2 \theta \, (k_{zb} - k_{yb})$$

$$K^{ww\theta} = k_{yh} + k_{yb} + \sin^2 \theta \, (k_{zb} - k_{yb}) \qquad (26)$$

$$k^{vw\theta} = (k_{zb} - k_{yb}) \sin \theta \cos \theta$$

where the stiffness coefficients, the k's are independent of pitch angle. Note that the effective spring constants of the hub k_{zh} and k_{zb} appear as a sum. This result is of a form that would be expected for two springs with spring constants k_{zh} and k_{zb} connected in parallel.

This result can be written in matrix notation by defining three matrices

$$k_H \equiv \begin{bmatrix} k_{zh} & 0 \\ 0 & k_{yh} \end{bmatrix}$$

$$k'_B \equiv \begin{bmatrix} k_{zb} & 0 \\ 0 & k_{yb} \end{bmatrix}$$

$$\theta \equiv \begin{bmatrix} \cos\theta & \sin\theta \\ -\sin\theta & \cos\theta \end{bmatrix}$$

The stiffness matrix may be written as

$$[k] = [k_H] + [\theta]^{-1} [k'_B] [\theta] \qquad (27)$$

where all of the effects of blade pitch are contained in the rotation matrix $[\theta]$. Thus this displays in convenient form the stiffness matrix for the flexible blade model in the case in which it is assumed that the mode shapes are independent of pitch and are the same for both deflections. There are five parameters involved in this form to define the coefficients in the stiffness matrix. The four stiffness coefficients and the pitch angle θ.

The number of independent parameters in the stiffness matrix can be

reduced by one by introducing the concept of a principal axis, that is by finding the transformation which diagonalizes the above matrix and then expressing the rotation of the principal axis in terms of the pitch angle. Consider therefore, a rotation matrix $[\gamma]$ which diagonalizes k by a similarity transformation

$$[K] \equiv [\gamma]^{-1} [k] [\gamma]$$

If the matrix [k] is denoted as

$$k \equiv \begin{bmatrix} k_{11} & k_{12} \\ k_{12} & k_{22} \end{bmatrix}$$

the rotation which diagonalizes the matrix k is γ_p where (cf. (23))

$$\tan 2\gamma_p = \frac{2\, k_{12}}{k_{11} - k_{22}} = \frac{\Delta k_b \sin 2\,\theta}{\Delta k_h + \Delta k_b \cos 2\theta} \tag{28}$$

where

$$\Delta k_b \equiv (k_{zb} - k_{yb})$$

$$\Delta k_h \equiv (k_{zh} - k_{yh})$$

γ_p is the rotation of the principal axis which is given above as a function of the blade pitch angle and the various stiffnesses. It can be noted that if the blade stiffness is equal in both directions then the principal axis does not rotate with blade pitch. If the hub stiffness is equal in both directions then the rotation of the principal axis is equal to change in pitch angle.

The stiffness coefficients in the diagonalized matrix are:

$$K_{11} = \frac{1}{2}(\Sigma k_h + \Sigma k_b) + \frac{1}{2}\left(\frac{\Delta k_h + \Delta k_b \cos 2\theta}{\cos 2\gamma_p}\right)$$

$$K_{22} = \frac{1}{2}(\Sigma k_h + \Sigma k_b) - \frac{1}{2}\left(\frac{\Delta k_h + \Delta k_b \cos 2\theta}{\cos 2\gamma_p}\right) \qquad (29)$$

where

$$\Sigma k_h \equiv (k_{zh} + k_{yh}) \qquad \Sigma k_b \equiv (k_{zb} + k_{yb})$$

It can be seen that if the blade stiffnesses are equal then these two stiffness coefficients are independent of pitch angle. Similarly if the hub stiffnesses are equal these coefficients are independent of pitch. That is, in both these limiting cases, the two nonrotating natural frequencies of the blades will be independent of blade pitch.

Now these results are compared to rigid blade models with root springs which may be assumed to represent the structural characteristics of the blades for use in an analysis of flap-lag stability in a somewhat simpler fashion. It will be shown that the spring model prposed in Reference 1 gives rise to a different pitch dependence from that given by the stiffness matrix of equation (27).

Therefore, two spring models will be considered, the one proposed by Ormiston (Reference 1) which will be referred to as the series spring model and a second one referred to as the parallel spring model. These two models will be compared to the results obtained from the flexible blade assuming that the mode shapes are independent of pitch angle. Particular interest

centers around the manner in which the results depend upon pitch angle.

Consider the structural properties of the hub to be represented by two orthogonal springs which produce moments proportional to deflection in an axis system parallel to the perpendicular to the shaft. The structural properties of the blade are represented by two orthogonal springs outboard of the hub which are aligned parallel and perpendicular to the chord line of the blade (precisely speaking the principal axes of the blade). In order to make the notation somewhat more compact the subscripts 1 and 2 refer to the two directions. A primed quantity is referenced to the blade axis system and an unprimed quantity is referenced to the hub axis system. Therfore, the stiffness matrices are

$$K_H \equiv \begin{bmatrix} K_{H_{11}} & 0 \\ 0 & K_{H_{22}} \end{bmatrix} \qquad K'_B \equiv \begin{bmatrix} K'_{B_{11}} & 0 \\ 0 & K'_{B_{22}} \end{bmatrix}$$

where these stiffness coefficients are independent of pitch. The deflections about these two axes are denoted as follows

$$\{\phi_H\} \equiv \begin{Bmatrix} \phi_{H_1} \\ \phi_{H_2} \end{Bmatrix} \qquad \{\phi'_B\} \equiv \begin{Bmatrix} \phi'_{B_1} \\ \phi'_{B_2} \end{Bmatrix}$$

and of course $\{\phi'_H\}$ denotes the hub deflection in the blade axis system and $\{\phi_B\}$ the blade deflection in the hub axis system. These angles are assumed small so that it is not necessary to introduceEuler angles. Figure 14 shows the definitions of these quantities. These quantities are related

by the rotation matrix

$$[\theta] \equiv \begin{bmatrix} \cos\theta & \sin\theta \\ -\sin\theta & \cos\theta \end{bmatrix}$$

so that

$$\begin{aligned} \{\phi'_B\} &= [\theta] \{\phi_B\} \\ \{\phi'_H\} &= [\theta] \{\phi_H\} \end{aligned} \tag{30}$$

The potential energy of this spring system can be written as (Meirovitch[3])

$$V = \frac{1}{2} \{\phi_H\}^T [K_H] \{\phi_H\} + \frac{1}{2} \{\phi'_B - \phi'_H\}^T [K'_B] \{\phi'_B - \phi'_H\} \tag{31}$$

where the superscript T indicates the transpose of the matrix.

The coordinates in the second term are expressed in terms of coordinates in the hub system using the transformation (30)

$$V = \frac{1}{2} \{\phi_H\}^T [K_H] \{\phi_H\} + \frac{1}{2} \{\phi_B - \phi_H\}^T [\theta]^T K'_B] [\theta] \{\phi_B - \phi_H\} \tag{32}$$

where the notation

$$[K_B] \equiv [\theta]^T [K'_B] [\theta]$$

is introduced such that

$$V = \frac{1}{2} \{\phi_H\}^T [K_H] \{\phi_H\} + \frac{1}{2} \{\phi_B - \phi_H\}^T [K_B] \{\phi_B - \phi_H\} \tag{33}$$

In this expression for potential energy there are four degrees-of-freedom the blade deflection in two directions $\{\phi_B\}$ and the hub deflection in two directions $\{\phi_H\}$. The two spring models to be discussed involve different assumptions as to the relationship between these degrees-of-freedom. Two spring models are developed to show clearly the analog between the fixed mode analysis and a rigid blade model with root springs. The parallel

spring model is developed with the specific objective of obtaining a stiffness matrix which varies in the same fashion with pitch angle as the fixed mode analysis (Equation (27)).

The parallel spring model consists of making the assumption that the hub deflections are proportional to the blade deflections

$$\{\phi_H\} = [\alpha]\ \{\phi_B\} \tag{34}$$

such that

$$V = \frac{1}{2}\{\phi_B\}^T [\alpha]^T [K_H] [\alpha] \{\phi_B\} + \frac{1}{2}\{\phi_B\}^T ([I] - [\alpha])^T [K_B] ([I] - [\alpha])\ \{\phi_B\} \tag{35}$$

and the stiffness terms are therefore

$$\{\frac{\partial V}{\partial \phi_B}\} = [\alpha]^T [K_H] [\alpha] \{\phi_B\} + ([I] - [\alpha])^T [K_B] ([I] - [\alpha])\ \{\phi_B\} \tag{36}$$

In the parallel spring model it is further assumed that the α matrix involves only one constant such that

$$[\alpha] = \alpha\ [I] \tag{37}$$

and therefore, the stiffness terms for the parallel spring model are

$$\{\frac{\partial V}{\partial \phi_B}\}_p = \alpha^2\ [\bar{\bar{K}}_H] + (1 - \alpha)^2\ [\bar{\bar{K}}_B] \tag{38}$$

where the bars are introduced to indicate that this is the result for the parallel spring model. The pitch angle dependence is contained in $[\bar{\bar{K}}_B]$ only where

$$[\bar{\bar{K}}_B] = [\theta]^{-1}\ [\bar{\bar{K}}'_B]\ [\theta]$$

Thus the assumption that the hub deflections are proportional to blade deflections and are independent of stiffness yields a stiffness matrix that has the identical pitch dependence as the flexible blade model with

fixed mode shapes (Equation (27)).

The series spring model is obtained by allowing $\{\phi_B\}$ and $\{\phi_H\}$ to be independent and determining the relationship between these two variables from the potential energy expression assuming that the inboard segment, i.e., the hub, has no mass such that in effect the matrix $[\alpha]$ is found from the following conditions:

$$\{\frac{\partial V}{\partial \phi_H}\} = 0 \tag{39}$$

From (39), using (33)

$$\{\frac{\partial V}{\partial \phi_H}\} = [K_H] \{\phi_H\} - [K_B] \{\phi_B - \phi_H\} = 0 \tag{40}$$

Therefore

$$\{\phi_H\} = [K_H + K_B]^{-1} [K_B] \{\phi_B\} \tag{41}$$

that is for the series spring model, cf. (34) and (41),

$$[\alpha] = [K_H + K_B]^{-1} [K_B] \tag{42}$$

Also

$$[\alpha]^T = [K_B] [K_H + K_B]^{-1} \tag{43}$$

since $[K_H + K_B]$ and $[K_B]$ are symmetric. Now from (36)

$$\{\frac{\partial V}{\partial \phi_B}\} = ([\alpha]^T [K_H + K_B] [\alpha] + [K_B] - [\alpha]^T [K_B] - [K_B] [\alpha]) \{\phi_B\}$$

using (42) and (43)

$$= [K_B] [K_H + K_B]^{-1} [K_B] + [K_B] - 2 [K_B] [K_H + K_B]^{-1} [K_B] \{\phi_B\}$$

$$= [K_B] ([I] - [K_H + K_B]^{-1} [K_B]) \{\phi_B\}$$

Hence

$$\left\{\frac{\partial V}{\partial \phi_B}\right\}_S = [K_B]\,[K_H + K_B]^{-1}\,[K_H]\,\{\phi_B\} \tag{44}$$

Thus this is the form of the stiffness terms for the series spring model where again the stiffness dependence on pitch angle is given by $[K_B]$ which is equal to

$$[K_B] = [\theta]^{-1}\,[K'_B]\,[\theta]$$

Thus, to summarize, the stiffness matrix for the parallel spring model is

$$[K]_P = \alpha^2\,[\bar{\bar{K}}_H] + (1-\alpha)^2\,[\bar{\bar{K}}_B] \tag{45}$$

and the series spring model

$$[K]_S = [K_B]\,[K_H + K_B]^{-1}\,[K_H] \tag{46}$$

To show the manner in which the series stiffness matrix varies with pitch the series spring model can be written as follows, noting that det K_B = det K'_B since $[K_B]$ and $[K'_B]$ are related by a similarity transformation,

$$[K]_S = \left(\frac{\det K'_B}{\det (K_H + K'_B)}\,[K_H] + \frac{\det K_H}{\det (K_H + K'_B)}\,[K_B]\right)\left(\frac{1}{1 + \dfrac{\Delta K_H\,\Delta K'_B}{\det (K_H + K_B')}\sin^2\theta}\right) \tag{47}$$

It can be seen that the first term in parentheses, (47), gives the same pitch dependence to the stiffness terms as found in the parallel spring. The second term in this expression gives rise to an additional pitch dependence which is a function of the product of the blade and hub stiffness differences.

Now, compare these results to those obtained from the flexible blade model with fixed mode shapes which are independent of pitch. This stiffness matrix is of the form

$$[k] = [k_H] + [\theta]^{-1} [k'_\beta] [\theta] \tag{27}$$

The same dependence with pitch angle is found as for the parallel spring model as would be expected physically from the assumption of fixed mode shapes, see (45). The matrix $[\bar{\bar{K}}_\beta]$ has the form

$$[\bar{\bar{K}}_\beta] = \begin{bmatrix} K'_{\beta_{11}} - \Delta K'_\beta \sin^2\theta & \Delta K'_\beta \sin\theta \cos\theta \\ \Delta K'_\beta \sin\theta \cos\theta & K'_{\beta_{22}} + \Delta K'_\beta \sin\theta \end{bmatrix} \tag{48}$$

Thus if the blade stiffnesses are equal then all three of these expressions give stiffness matrices which are independent of blade pitch. If the hub stiffnesses are equal again all three of these results agree as to the pitch dependence of the stiffness terms. In the general case in which both stiffnesses are unequal the series spring model yields a different variation of stiffness with pitch from the other two.

It is further interesting to note that both the series and the parallel spring models give the same principal axis dependence upon pitch since the difference between the parallel spring model and the series

spring model is multiplication of all terms in the series spring stiffness matrix by the single factor

$$\left(\frac{1}{1 + \dfrac{\Delta K_H \ \Delta K_B'}{\det (K_H + K_B')} \sin^2 \theta} \right)$$

The equivalence between the various models is as follows. For the elastic model to be equivalent to the parallel spring model, we require

$$\begin{aligned} k_{H_{11}} &= \alpha^2 \bar{\bar{K}}_{H_{11}} \\ k_{H_{22}} &= \alpha^2 \bar{\bar{K}}_{H_{22}} \\ k_{B_{11}}' &= (1 - \alpha)^2 \bar{\bar{K}}_{B_{11}}' \\ k_{B_{22}}' &= (1 - \alpha)^2 \bar{\bar{K}}_{B_{22}}' \end{aligned} \tag{49}$$

where the parameter α is arbitrary.

For the elastic model to be equivalent to the series spring model, noting that

$$\frac{\det K_B'}{\det (K_H + K_B')} = \delta \epsilon \qquad \text{and} \qquad \frac{\det K_H}{\det (K_H + K_B')} = (1 - \delta)(1 - \epsilon)$$

where

$$\delta \equiv \frac{K_{B_{11}}'}{K_{B_{11}}' + K_{H_{11}}} \qquad \epsilon \equiv \frac{K_{B_{22}}'}{K_{B_{22}}' + K_{H_{22}}}$$

We require

$$\begin{aligned} k_{H_{11}} &= \delta \epsilon K_{H_{11}} \\ k_{H_{22}} &= \delta \epsilon K_{H_{22}} \\ k_{B_{11}}' &= (1 - \delta)(1 - \epsilon) K_{B_{11}}' \\ k_{B_{22}}' &= (1 - \delta)(1 - \epsilon) K_{B_{22}}' \end{aligned} \tag{50}$$

Recall that this equivalence does not account for the multiplying factor noted above which is a function of the pitch angle. This equivalence will give the same principal axis direction for either model. However, the dependence of natural frequency on pitch angle will be different.

These equations give the following relationships between spring constants.

$$K_{H_{22}} = \left(\frac{k_{H_{22}}}{k_{H_{11}}}\right) K_{H_{11}}$$

$$K_{\beta_{11}}' = \left(\frac{k_{H_{22}}}{k_{\beta_{22}}'}\right) K_{H_{11}} \qquad (51)$$

$$K_{\beta_{22}}' = \left(\frac{k_{H_{22}}}{k_{\beta_{11}}'}\right) K_{H_{11}}$$

$$K_{H_{11}} = \frac{(k_{H_{11}} + k_{\beta_{11}}')(k_{H_{22}} + k_{\beta_{22}}')}{k_{H_{22}}'}$$

Thus given the results of the flexible blade calculation, equations (25)-(27), the spring constants to be used in the series spring model are determined by

$$K_{H_{11}} = (k_{H_{11}} + k_{\beta_{11}}') \left(1 + \frac{k_{\beta_{22}}'}{k_{H_{22}}}\right)$$

$$K_{H_{22}} = (k_{H_{22}} + k_{\beta_{22}}') \left(1 + \frac{k_{\beta_{11}}'}{k_{H_{11}}}\right) \qquad (52)$$

$$K_{B'_{11}} = (k_{H_{11}} + k_{B'_{11}}) \left(1 + \frac{k_{H_{22}}}{k_{B'_{22}}}\right)$$

$$K_{B'_{22}} = (k_{H_{22}} + k_{B'_{22}}) \left(1 + \frac{k_{H_{11}}}{k_{B'_{11}}}\right)$$

The correspondence between the notation used here and that of Ormiston/Bousman[2] is

$$R_\zeta = (1 - \delta)$$

$$R_\beta = (1 - \epsilon)$$

$$K_\zeta = \frac{K'_{B_{11}} K_{H_{11}}}{K_{B'_{11}} + K_{H_{11}}} \tag{53}$$

$$K_\beta = \frac{K'_{B_{22}} K_{H_{22}}}{K_{B'_{22}} + K_{H_{22}}}$$

Expressing Ormiston's parameters[1,2] in terms of the elastic model with fixed mode shapes (equations (25) - (27))

$$R_\zeta = \frac{k_{B'_{22}}}{k_{H_{22}} + k_{B'_{22}}}$$

$$R_\beta = \frac{k'_{B_{11}}}{k'_{B_{11}} + k_{H_{11}}}$$

$$\omega_\zeta^2 = (k'_{B_{11}} + k_{H_{11}})$$

$$\omega_\beta^2 = (k'_{B_{22}} + k_{H_{22}})$$

$$R = \frac{k_{\beta'_{11}} - k_{\beta'_{22}}}{(k_{\beta'_{11}} - k_{\beta'_{22}}) + (k_{H_{11}} - k_{H_{22}})} \tag{54}$$

The factor missing in the elastic model with fixed mode shapes is

$$\left(1 + \frac{(k_{H_{11}} - k_{H_{22}})\,(k_{\beta'_{11}} - k_{\beta'_{22}})}{(k_{H_{11}} + k_{\beta'_{11}})\,(k_{H_{22}} + k_{\beta'_{22}})} \sin^2\theta\right)^{-1}$$

The factor within the parentheses is Δ in Ormiston's notation.

Using the above equivalences, consider the nonrotating natural frequencies and the differences which arise from the two approaches. Recall that both models give the same rotation of the principal axes with pitch angle.

The dependence of the nonrotating natural frequencies on pitch is given in the series spring case as

$$\omega_{1_s}^2, \omega_{2_s}^2 = -(2\omega_\zeta^2\ \omega_\beta^2)\left(\frac{1}{(\omega_\beta^2 + \omega_\zeta^2) \pm (\omega_\beta^2 - \omega_\zeta^2)\sqrt{1-4(R)(1-R)\sin^2\theta}}\right) \tag{55}$$

In the parallel spring (elastic model with fixed mode shapes) case,

$$\omega_{1_p}^2, \omega_{2_p}^2 = -\left(\frac{\omega_\zeta^2 + \omega_\beta^2}{2}\right) \pm \left(\frac{\omega_\beta^2 - \omega_\zeta^2}{2}\right)\sqrt{1 - 4\,(R)\,(1-R)\sin^2\theta} \tag{56}$$

These differ by the multiplying factor noted.

For a helicopter rotor where the blade pitch angle is small, it may be assumed that

$$4(R)\,(1-R)\sin^2\theta \ll 1$$

and the natural frequencies given by the two cases are approximately

$$\omega_{1_s}^2, \omega_{2_s}^2 \cong \omega_\zeta^2 \left\{ 1 - \left(\frac{\omega_\zeta^2}{\omega_\beta^2} - 1 \right) (R)\ (1-R)\ \theta^2 \right\}$$

$$\omega_\beta^2 \left\{ 1 - \left(\frac{\omega_\beta^2}{\omega_\zeta^2} - 1 \right) (R)\ (1-R)\ \theta^2 \right\}$$

$$\omega_{1_p}^2, \omega_{2_p}^2 \cong \omega_\zeta^2 \left\{ 1 + \left(\frac{\omega_\beta^2}{\omega_\zeta^2} - 1 \right) (R)\ (1-R)\ \theta^2 \right\}$$

$$\omega_\beta^2 \left\{ 1 + \left(\frac{\omega_\zeta^2}{\omega_\beta^2} - 1 \right) (R)\ (1-R)\ \theta^2 \right\}$$

The principal axis rotation given by both approaches is the same using the equivalences noted above. In terms of the elastic coupling parameter R,

$$\tan 2\gamma_p = \frac{R \sin 2\theta}{R \cos 2\theta + (1-R)}$$

The frequencies given by each approach in general is different. In the particular case where the ratio $\left(\frac{\omega_\zeta}{\omega_\beta}\right)^2$ is near to one, that is if $\left(\frac{\omega_\zeta}{\omega_\beta}\right)^2 = 1 + \eta$ where η is small compared to one then the same frequency dependence with pitch is obtained from both methods.

Thus using the equivalences given above to determine the corresponding parameters each model will give the same principal axis rotation, but the parallel spring and elastic blade model with mode shapes independent of pitch will give a different frequency variation with pitch from the series model.

Thus experiments to be described in a later report will not distinguish between the two approximations when the principal axis direction is measured.

Also if pitch angles typical of a helicopter are examined, only small changes in the frequency will be noted and it will be difficult to distinguish between these two approximation, series vs. parallel spring (or elastic blade model with mode shapes independent of pitch) from experimental results.

CONCLUSIONS

As a result of this analytical study of flap-lag stability in hovering flight the following conclusions can be drawn:

1.) Prediction of flap-lag stability is very sensitive to the assumptions used in modelling the aerodynamic and elastic characteristics of rotor blades.

2.) The equivalent lumped spring/mass model, determined from a single mode representation of the elastic deformation of a rotor blade/hub system in which the mode shapes are assumed to be independent of blade pitch, gives rise to a different dependence of the blade/hub stiffness matrix on blade pitch angle from the lumped model proposed in References 1 and 2.

3.) These two lumped spring/mass models, referred to as the parallel spring model (equivalent to the single mode analysis) and the series spring model (References 1 and 2) give identical results for the variation of the characteristic roots of flap-lag motion when the elastic coupling parameters R = 0 or 1 and different results for other values of R.

4.) It is possible to determine the equivalent lumped spring constants for either the parallel or series spring model from the results of an elastic analysis of a rotor blade.

5.) The elastic coupling parameter R can be conveniently interpreted as a measure of the rotation of the principal axis of the blade/hub system with blade pitch.

6.) Experimentally, the elastic coupling parameter R can be more precisely determined from principal axis measurements than from frequency measurements.

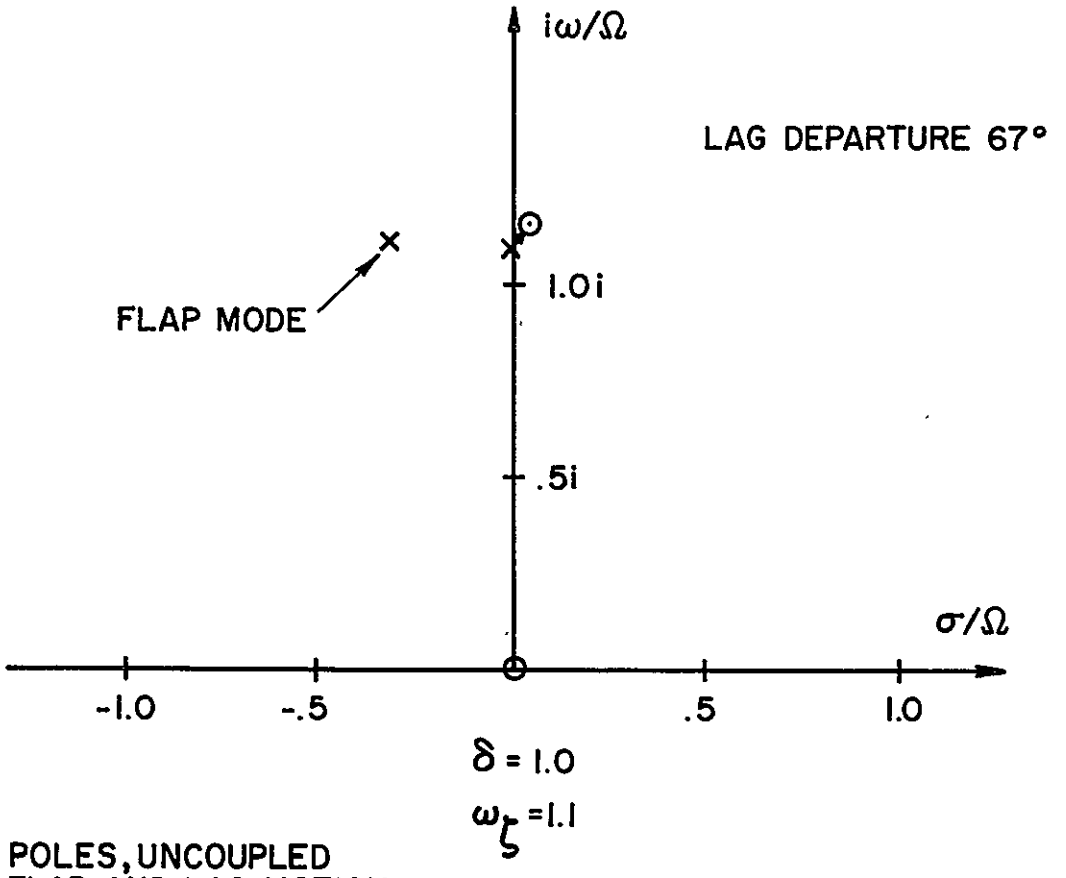

× = POLES, UNCOUPLED FLAP AND LAG MOTION

⊙ = ZEROS

$p^2 = 1.333$

$\gamma = 5$

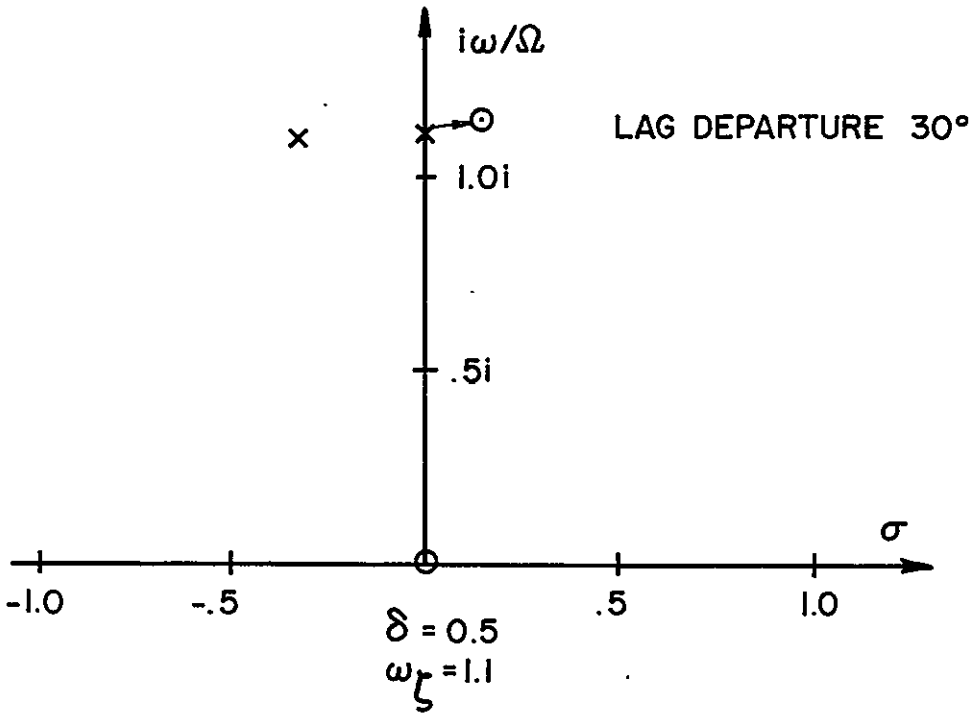

FIGURE 1. ROOT LOCUS FOR INCREASING PITCH ANGLE. NO ELASTIC COUPLING (R=0), $\omega_\zeta = 1.1$, INFLUENCE OF INFLOW APPROXIMATION.

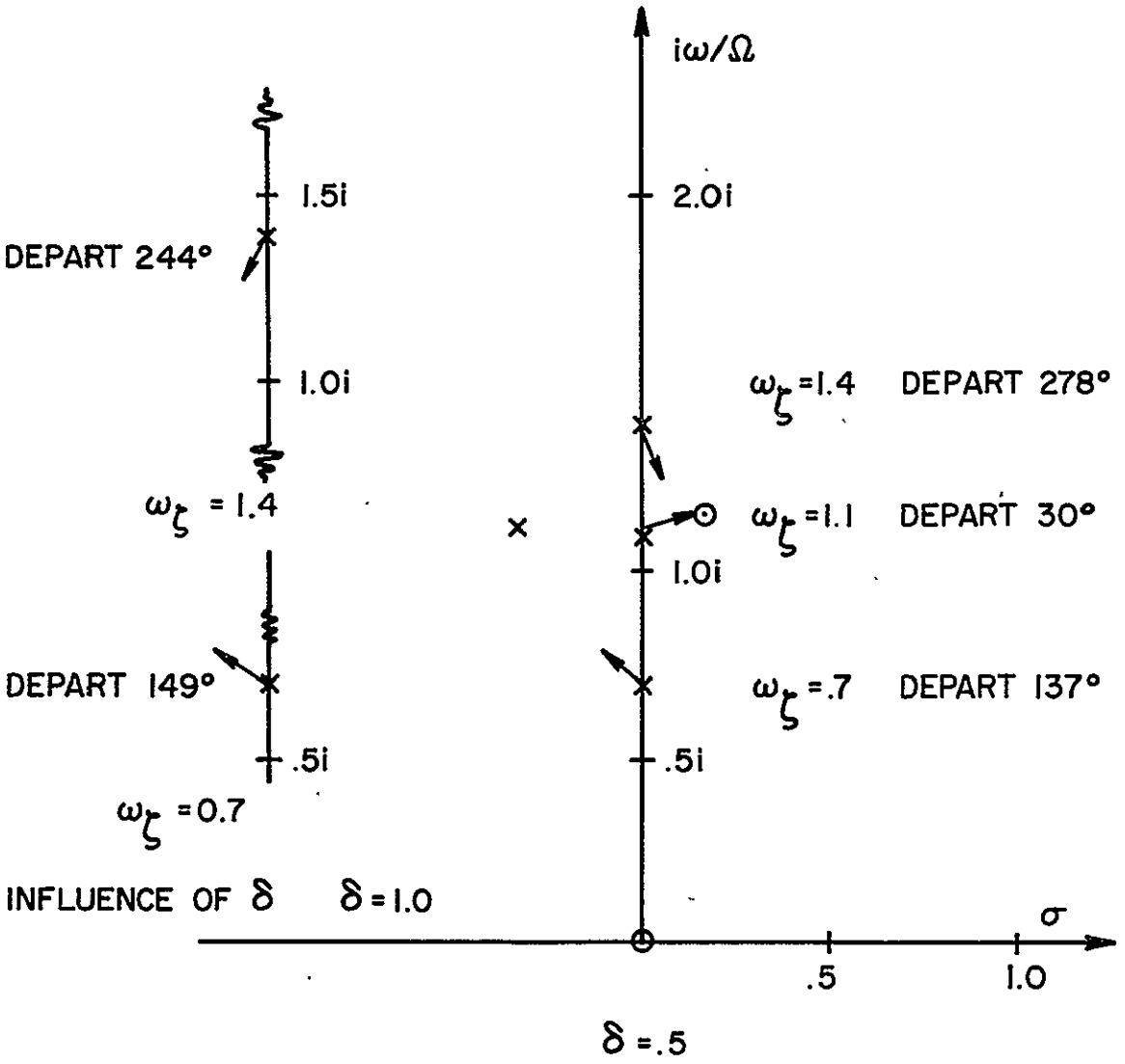

FIGURE 2. ROOT LOCUS FOR INCREASING PITCH ANGLE. NO ELASTIC COUPLING (R=0). VARIOUS ω_ζ.

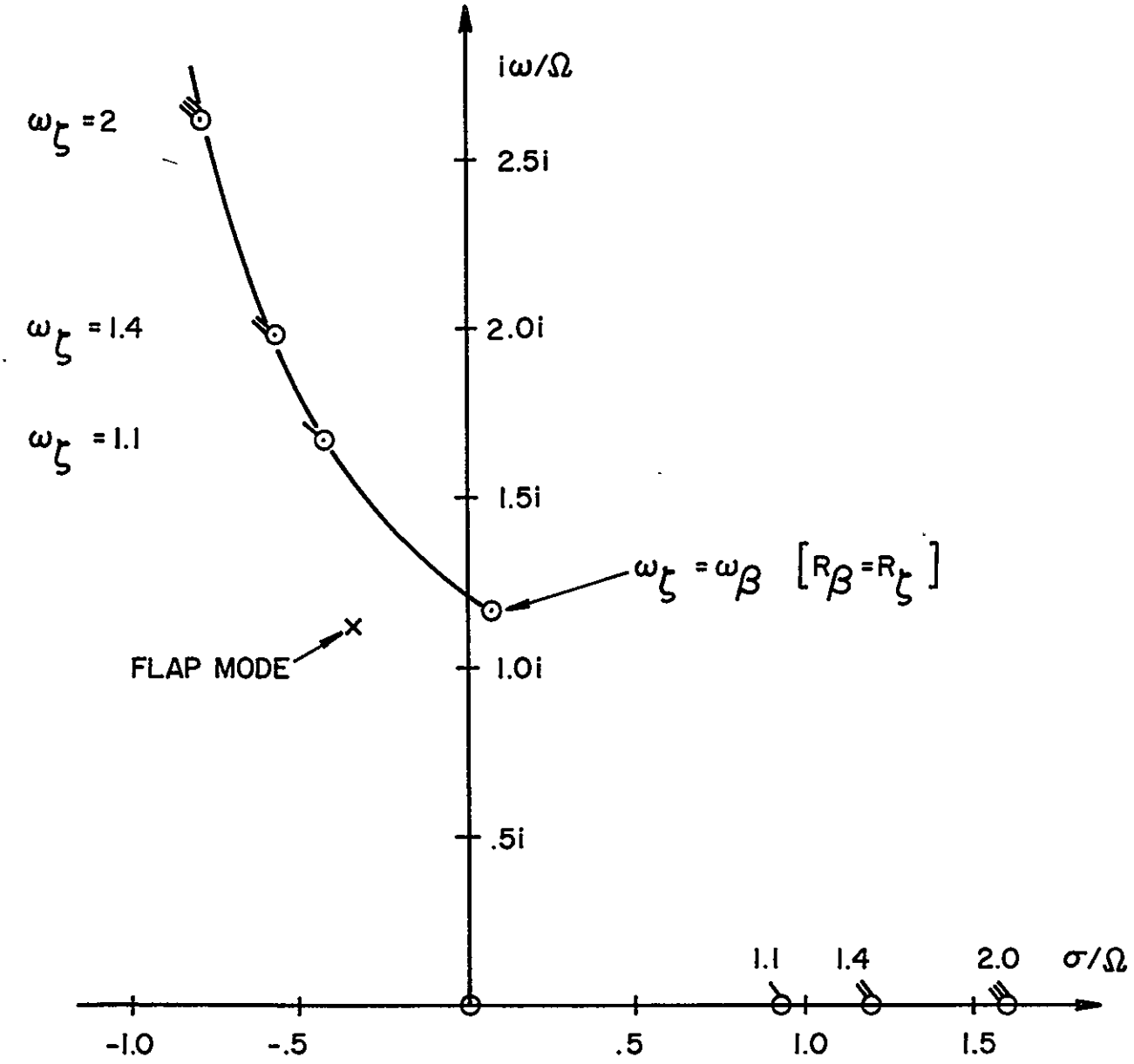

$p^2 = 1.33$

$\gamma = 5$

FIGURE 3. LOCUS OF ZEROS FOR INCREASING ω_ζ. FULL ELASTIC COUPLING (R=1), δ = 1.0

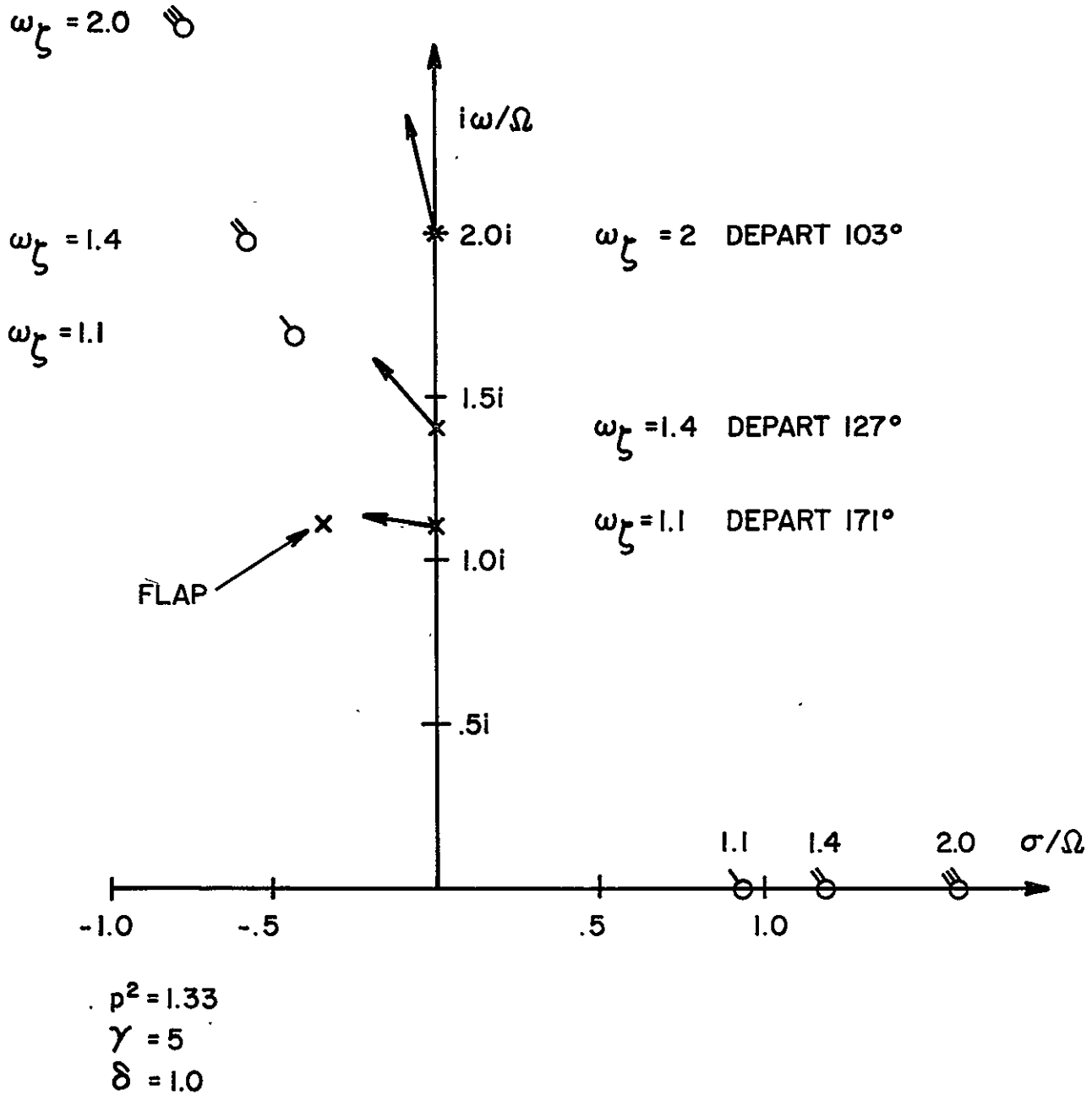

FIGURE 4. ROOT LOCUS FOR INCREASING PITCH ANGLE. FULL ELASTIC COUPLING (R = 1). VARIOUS ω_ζ.

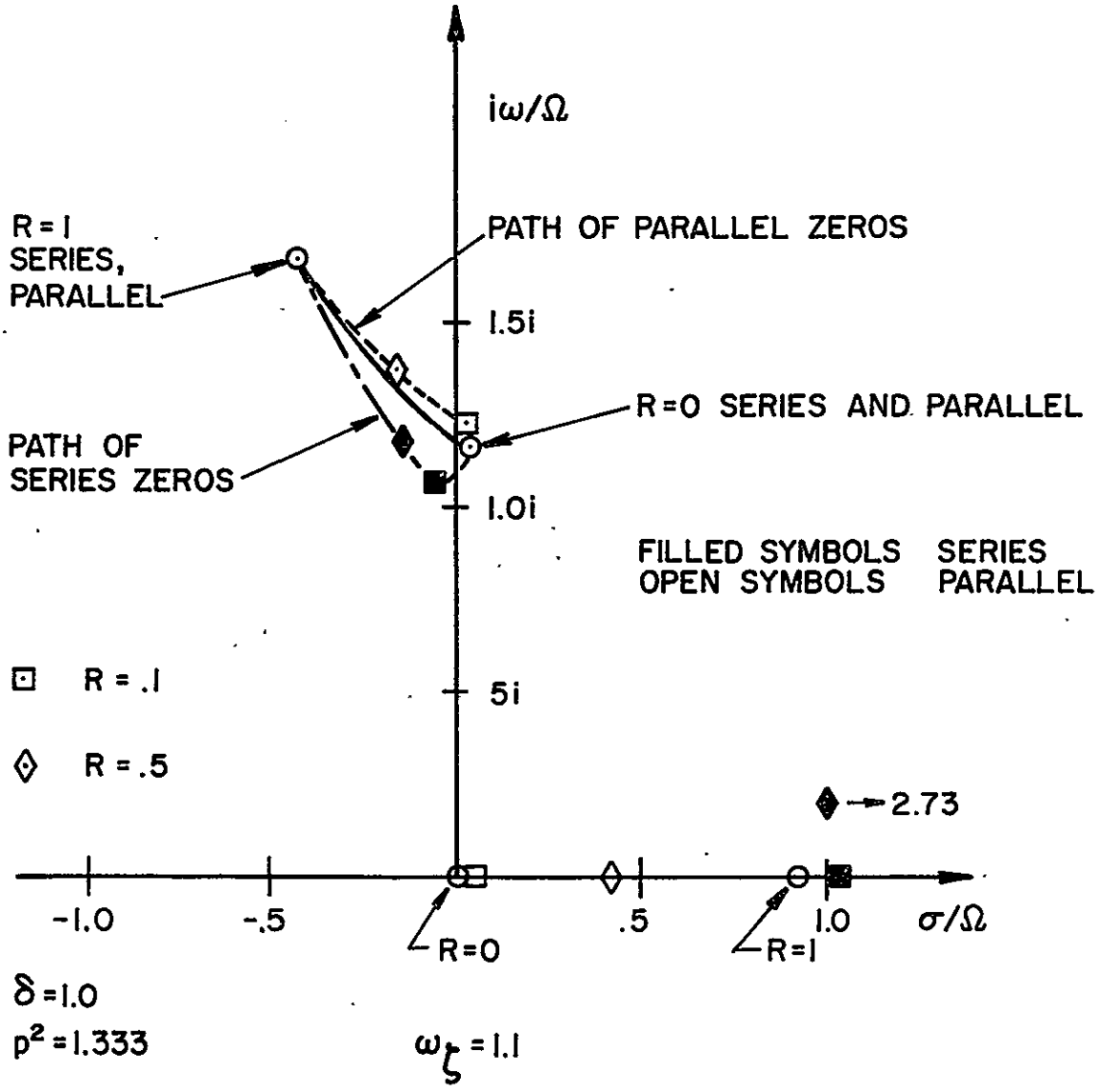

FIGURE 5. LOCUS OF ZEROS FOR INCREASING PITCH ANGLE AS A FUNCTION OF R FOR $\omega_\zeta = 1.1$

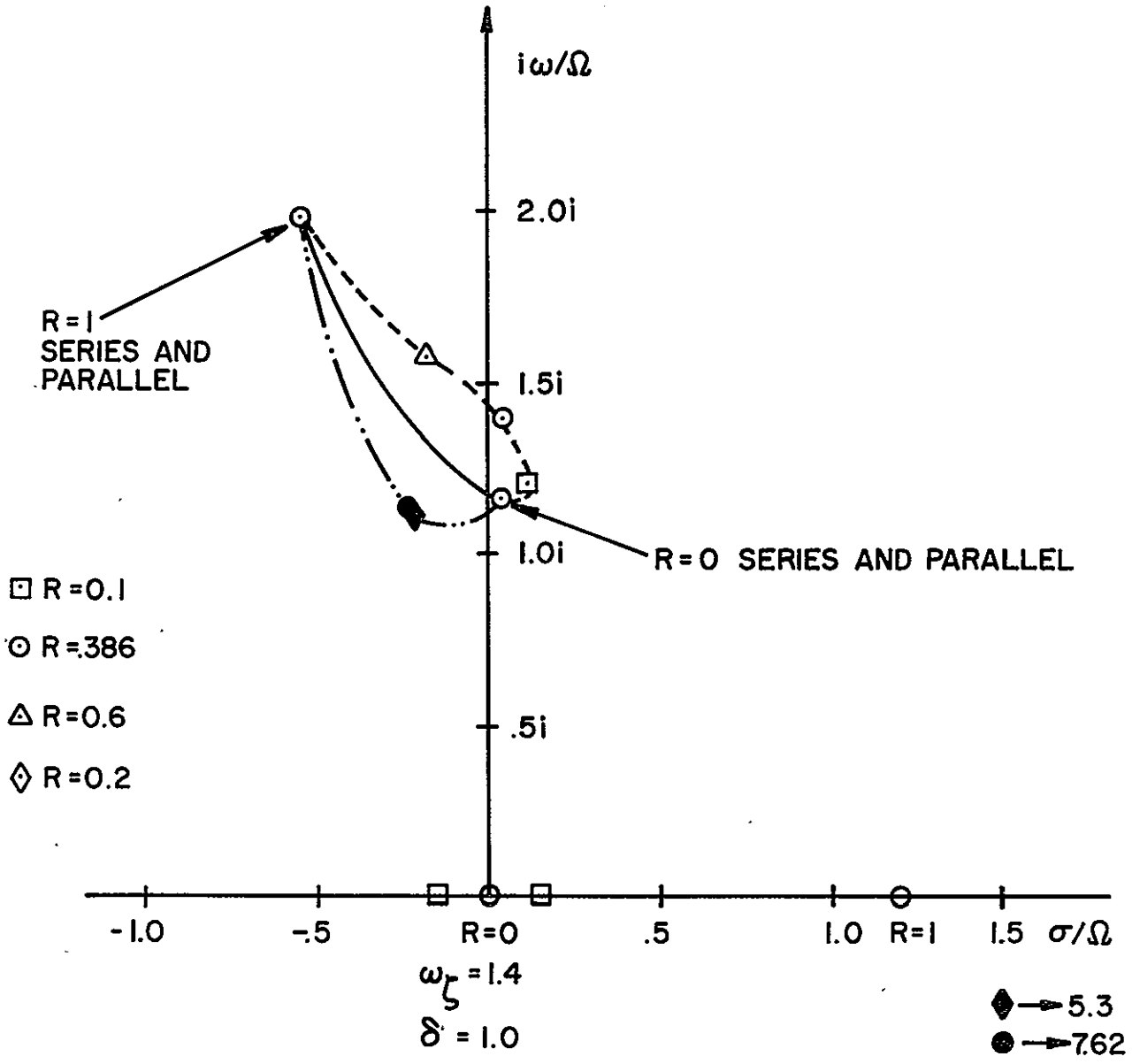

FIGURE 6. LOCUS OF ZEROS FOR INCREASING PITCH ANGLE AS A FUNCTION OF R FOR $\omega_\zeta = 1.4$.

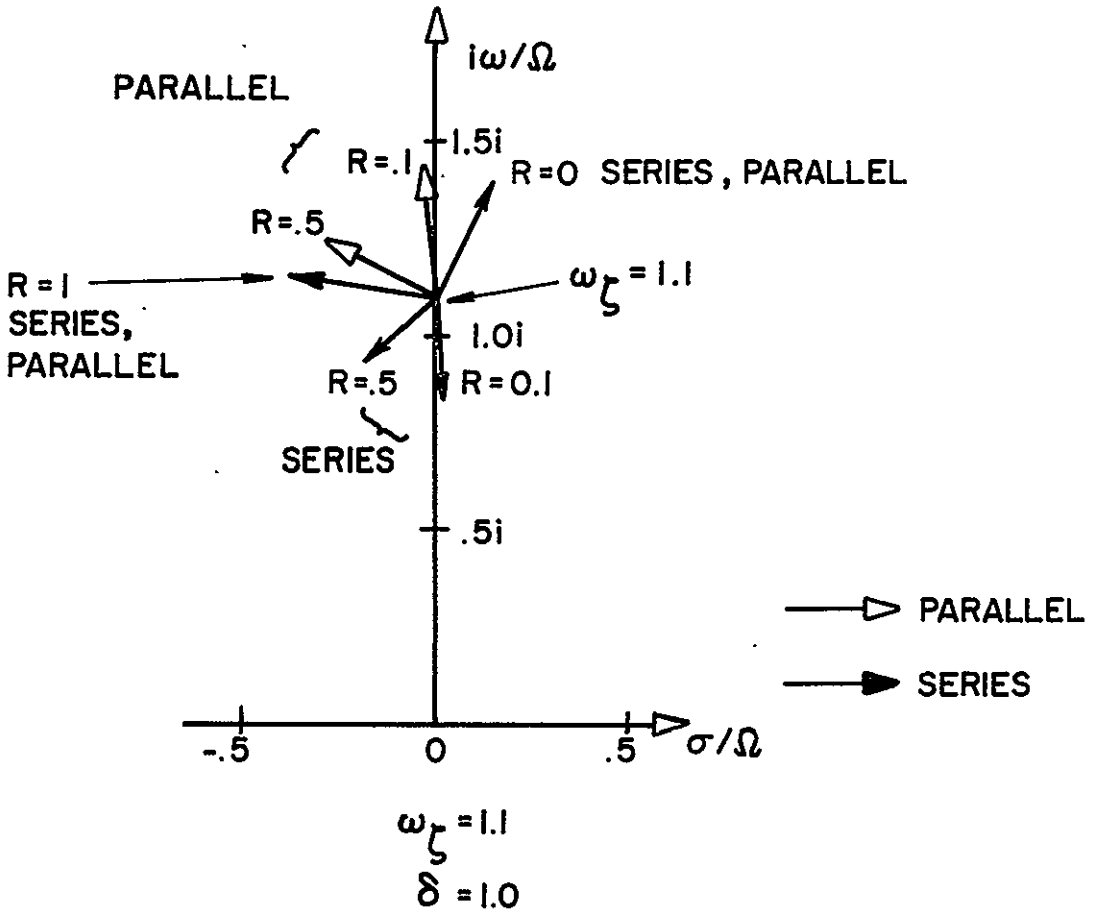

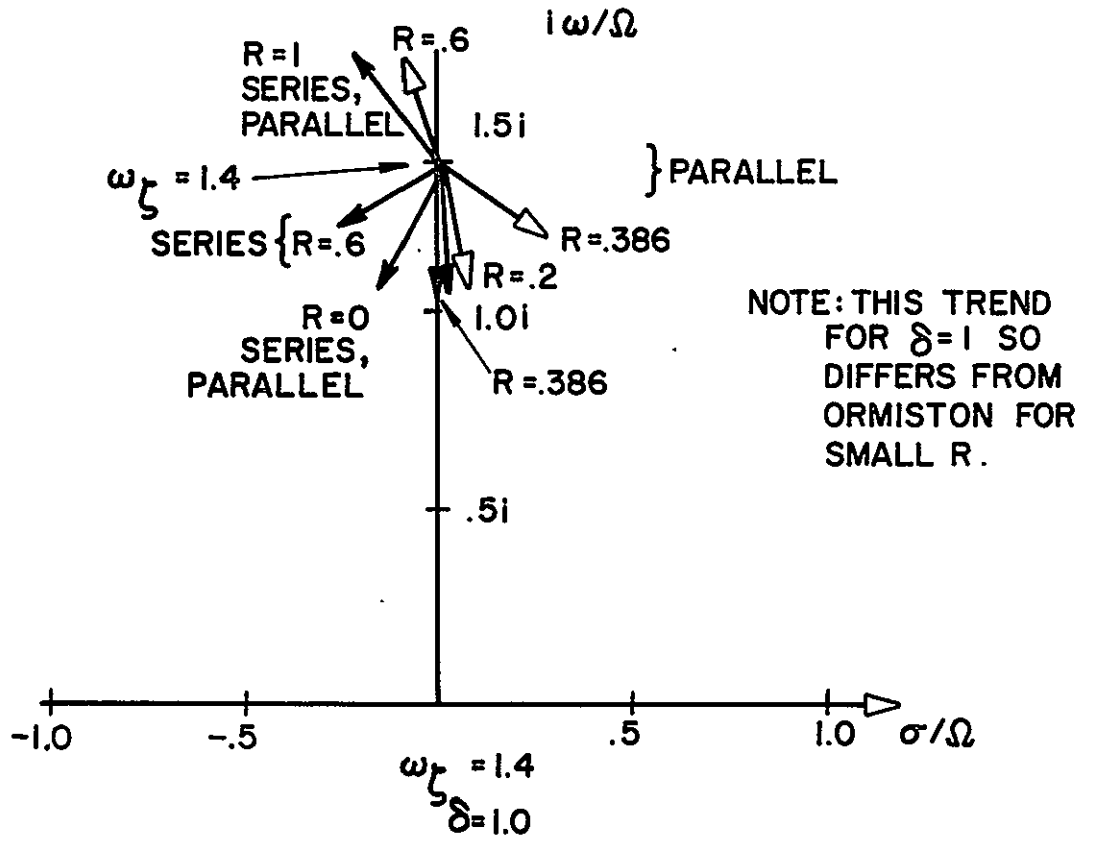

FIGURE 7. ROOT LOCUS DEPARTURE ANGLES AS A FUNCTION OF R FOR SERIES AND PARALLEL MODELS

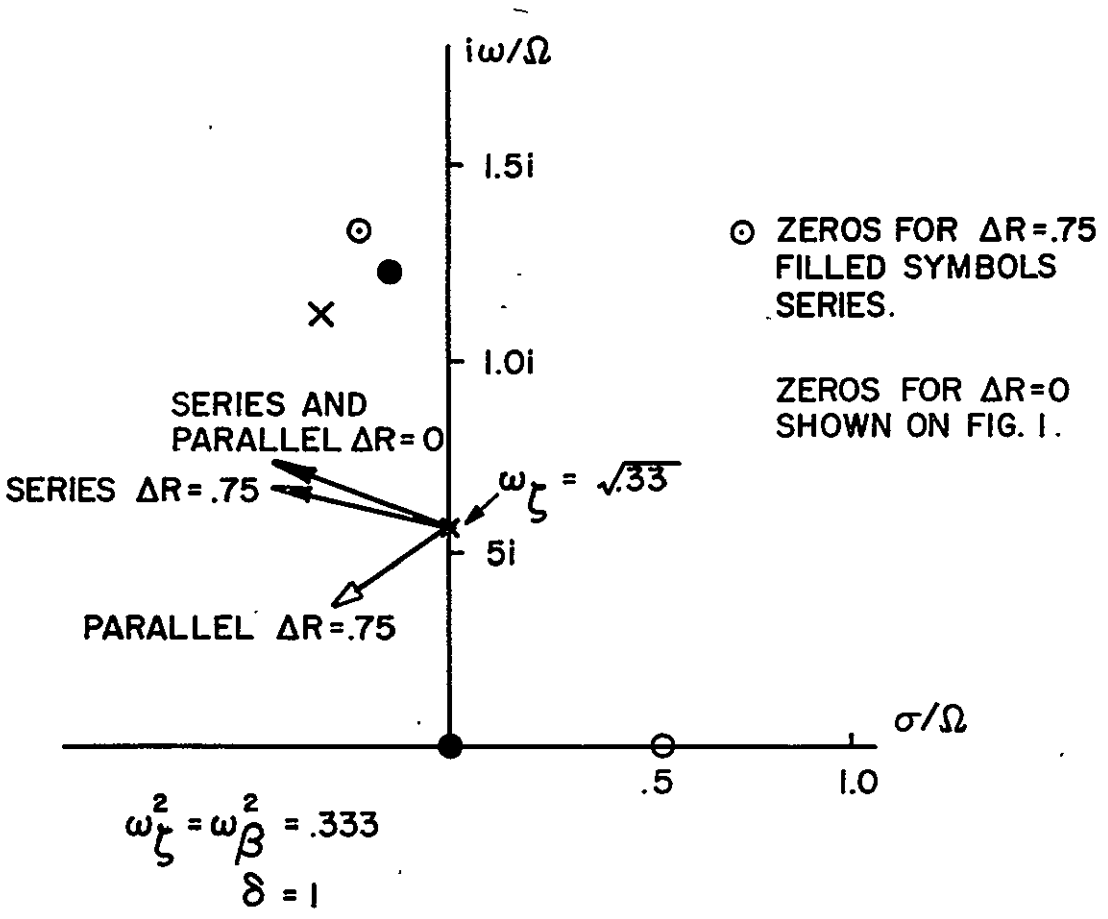

FIGURE 8. ROOT LOCUS FOR INCREASING PITCH ANGLE MATCHED STIFFNESS. COMPARISON OF SERIES AND PARALLEL MODELS.

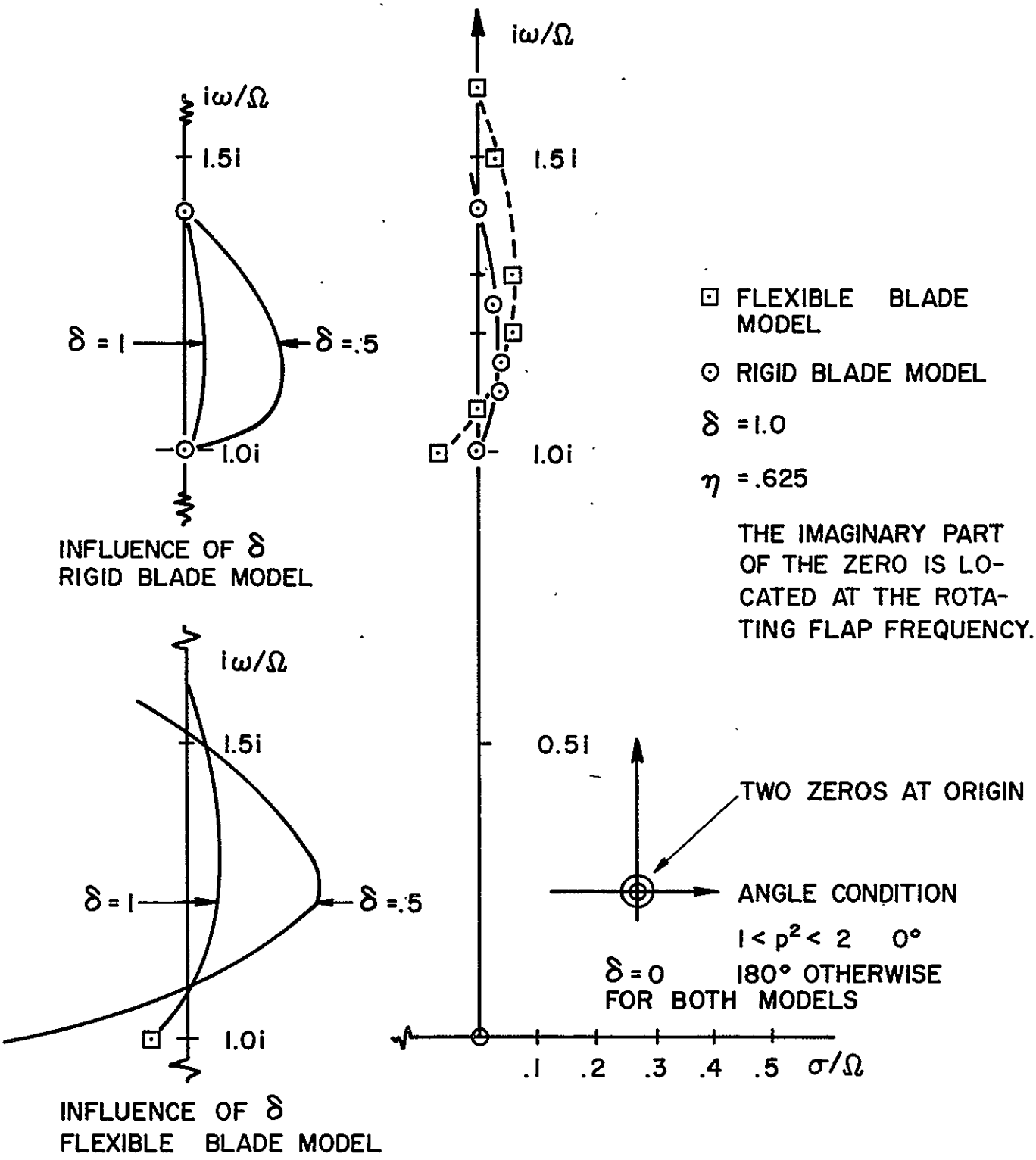

FIGURE 9. COMPARISON OF ZERO LOCATION FOR RIGID MODEL AND FLEXIBLE BLADE MODEL AS A FUNCTION OF FLAP FREQUENCY AND INFLOW PARAMETERS. ELASTICALLY UNCOUPLED R = 0.

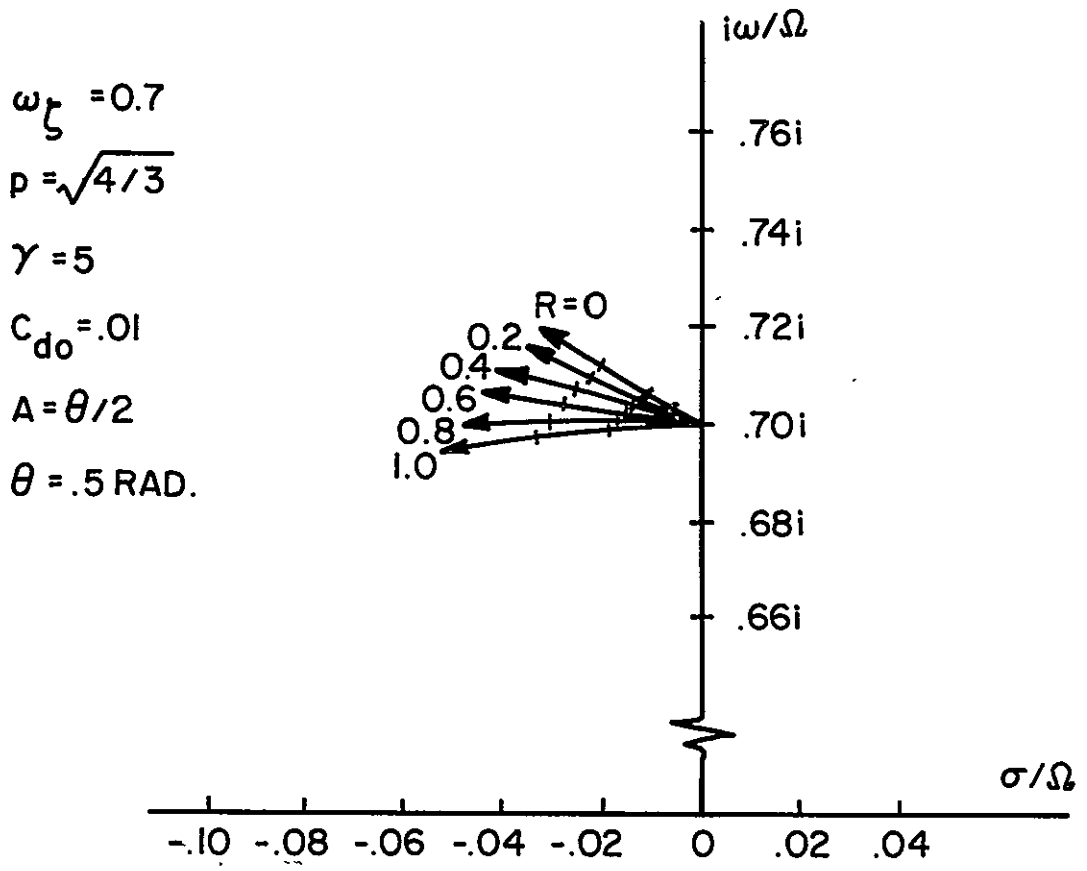

FIGURE 10. LOCUS OF LEAD-LAG ROOTS. VARIABLE ELASTIC COUPLING. PARALLEL SPRING MODEL

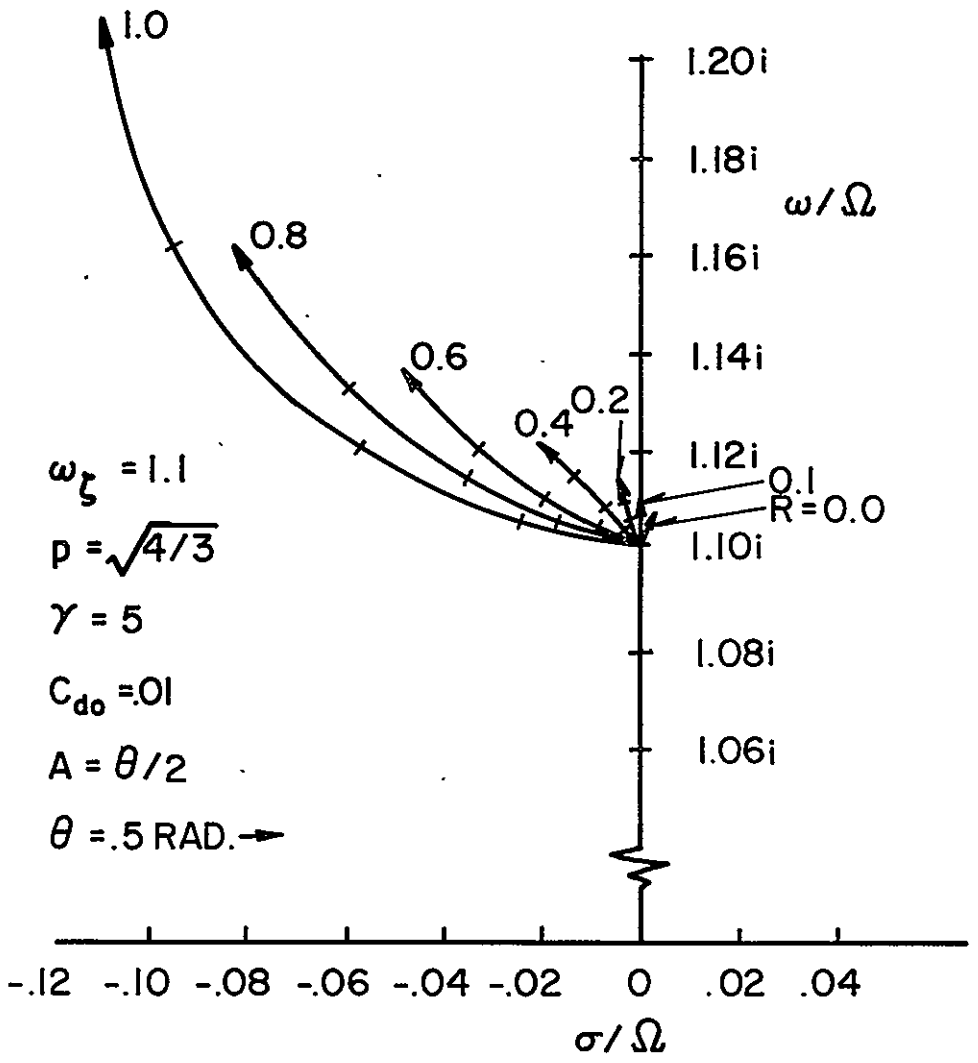

FIGURE 11. LOCUS OF LEAD-LAG ROOTS. VARIABLE ELASTIC COUPLING. PARALLEL SPRING MODEL

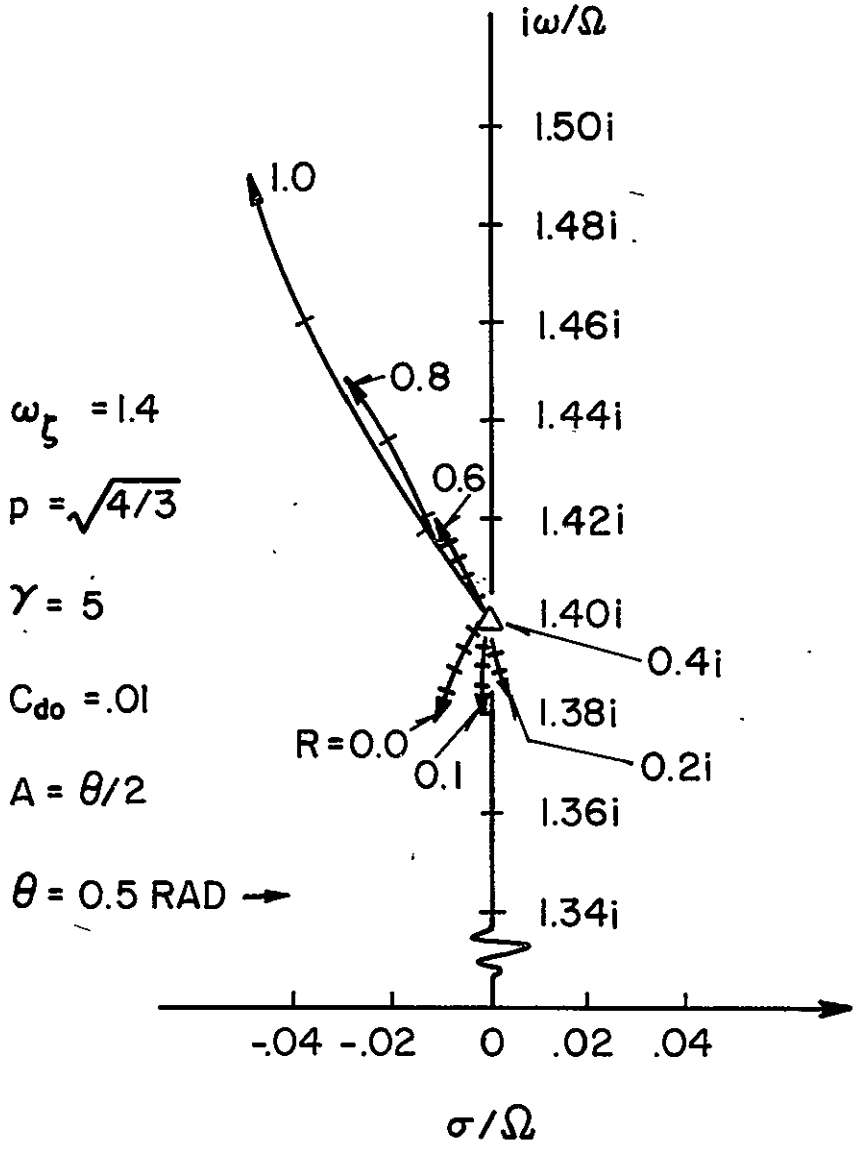

FIGURE 12. LOCUS OF LEAD-LAG ROOTS. VARIABLE ELASTIC COUPLING. PARALLEL SPRING MODEL

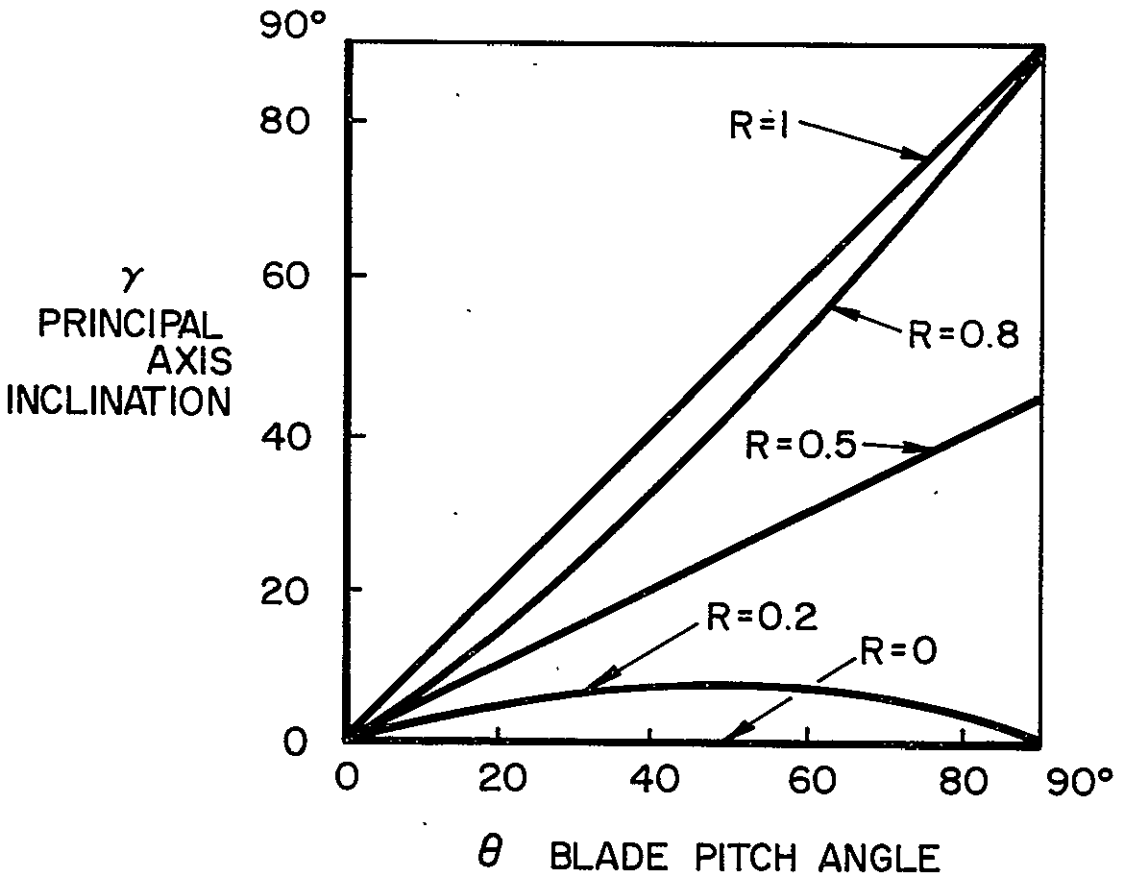

FIGURE 13. PRINCIPAL AXIS INCLINATION AS A FUNCTION OF BLADE PITCH ANGLE AND THE ELASTIC COUPLING PARAMETER R

REFERENCES

1. Ormiston, R. A. and Hodges, D. H.: "Linear Flap-Lag Dynamics of Hingeless Helicopter Rotor Blades in Hover", Journal of the American Helicopter Society, Vol. 17, No. 2, April 1972, pp. 2-14.

2. Ormiston, R. A. and Bousman, W. G.: "A Study of Stall-Induced Flap-Lag Instability of Hingeless Rotors", Journal of the American Helicopter Society, Vol. 20, No. 1, January 1975, pp 21-30.

3. Meirovitch, L.: Analytical Methods in Vibrations, MacMillan 1967.

4. Dowell, E. H.: "A Variational Rayleigh-Ritz Modal Approach for Non-Uniform Twisted Rotor Blades Undergoing Large Bending and Torsional Motion", Princeton University Aerospace and Mechanical Sciences Report No. 1193, November 1974.

APPENDIX I

FLAP-LAG EQUATIONS OF MOTION

The nonlinear equations of motion for a variable property rotor blade undergoing flap, lag and elastic twist deformations are developed in Reference 4 using a Rayleigh-Ritz procedure. Using a single mode for each type of deformation and ignoring elastic twist altogether we may write the modal equations for flap-lag motion as follows. It has been assumed in developing the aerodynamic forces that the induced velocity is independent of blade spanwise station. For convenience we have constructed nonlinear steady state (or static) equations and small perturbation (linear) dynamic equations about the steady state equilibrium. The latter are required for stability analysis.

STEADY STATE

$$v^{o}\left[M^{vv} + K^{Vv} + K^{vv\theta}\right] + w^{o}\,K^{vw\theta} = Q^{y^{o}}$$

$$M^{xw} + w^{o}\left[K^{Vw} + K^{ww\theta}\right] + v^{o}\,K^{vw\theta} = Q^{z^{o}}$$

PERTURBATION

$$\dot{v}\left[M^{uv\dot{v}v} + K^{V\dot{v}v}\right] v^{o} + \dot{w}\left[M^{uw\dot{w}v}\,w^{o} + M^{\dot{w}v}\right]$$

$$+ v\left[M^{vv} + K^{Vv} + K^{vv\theta}\right] + w\,K^{vw\theta} + M^{\dot{v}v}\,\ddot{v} = Q^{y}$$

$$\dot{v}\,[M^{\dot{v}w} + K^{V\dot{v}w}\,w^{o}] + w\,[K^{Vw} + K^{ww\theta}]$$

$$+ v\,K^{vw\theta} + M^{\ddot{w}w}\,\ddot{w} = Q^{z}$$

AERODYNAMIC FORCES

STEADY STATE

$$Q^{y^{o}} = -\rho\frac{ac}{2}\{\Omega\, v_{in}\, A^{x\theta v} - v_{in}^{2}\, A^{v} + \frac{C_{do}}{a}\,\Omega^{2}\, A^{xxv}\}$$

$$Q^{z^{o}} = -\rho\frac{ac}{2}\{-\Omega^{2}\, A^{xx\theta w} + \Omega\, v_{in}\, A^{xw}\}$$

PERTURBATION

$$Q^{y} = -\rho\frac{ac}{2}\{\dot{w}\,[\Omega\, A^{x\theta wv} - 2v_{in}\, A^{wv}] + \dot{v}\,[v_{in}\, A^{\theta vv} + 2\Omega\frac{C_{do}}{a}\, A^{xwv}]\}$$

$$Q^{z} = -\rho\frac{ac}{2}\{\dot{w}\,\Omega\, A^{xwv} + \dot{v}\,[v_{in}\, A^{vw} - 2\Omega\, A^{x\theta vw}]\}$$

The several inertial, stiffness and aerodynamic coefficient are given below. ψ_{v}, ψ_{w} are the lag and flap mode shapes assumed in the Rayleigh-Ritz analysis. Note that the mode shapes are dimensionless; however, $(\ )' = \frac{d}{dr}(\ )$.

MASS

$$M^{vv} = -\Omega^{2}\int_{o}^{R} m\,\psi_{v}^{2}\, dr$$

$$M^{\ddot{v}v} = \int_{o}^{R} m\,\psi_{v}^{2}\, dr$$

$$M^{\ddot{w}w} = \int_{o}^{R} m\,\psi_{w}^{2}\, dr$$

$$M^{\dot{v}w} = -M^{\dot{w}v} = 2\Omega\,\beta_{pc}\int_{o}^{R} m\,\psi_{v}\,\psi_{w}\, dr$$

$$M^{x\dot{w}} = \beta_{pc}\,\Omega^2 \int_o^R mr\,\psi_w \; dr$$

$$M^{uv\dot{v}v} = 2\,\Omega \int_o^R m\,C^{uv\dot{v}}\,\psi_v \; dr$$

$$M^{uw\dot{w}v} = 2\Omega \int_o^R m\,C^{uw\dot{w}}\,\psi_v \; dr$$

$$K^{V\dot{v}v} = \int_o^R C^{m\dot{v}}\,(\psi_v')^2 \; dr$$

$$K^{V\dot{v}w} = \int_o^R C^{m\dot{v}}\,(\psi_w')^2 \; dr$$

where

$$C^{m\dot{v}} = 2\Omega \int_r^R m\,\psi_v \, d\eta, \quad C^{uw\dot{w}} = -\int_o^r (\psi_w')^2 \, d\eta, \quad C^{uv\dot{v}} = -\int_o^r (\psi_v')^2 \, d\eta$$

Note that $K^{V\dot{v}v} = -M^{uv\dot{v}v}$, $M^{vv} = -\Omega^2 M^{\dot{v}v}$, $M^{ww} = -\Omega^2 M^{\dot{w}w}$

STIFFNESS

$$K^{Vv} = \int_o^R C^{mx}\,(\psi_v')^2 \; dr$$

$$K^{Vw} = \int_o^R C^{mx}\,(\psi_w')^2 \; dr$$

$$C^{mx} = \Omega^2 \int_r^R m\eta \, d\eta$$

$$K^{vv\theta} = \int_o^R [EI_{z'} \cos^2\theta + EI_{y'} \sin^2\theta]\,(\psi_v'')^2 \; dr$$

$$K^{ww\theta} = \int_o^R [EI_{z'} \sin^2\theta + EI_{y'} \cos^2\theta]\,(\psi_w'')^2 \; dr$$

$$K^{vw\theta} = K^{wv\theta} = \int_o^R [EI_{z'} - EI_{y'}] \frac{\sin 2\theta}{2}\,(\psi_v''\,\psi_w'') \; dr$$

θ is the rotation of the blade and in general consists of a constant part θ_o and a linear twist θ_1 such that

$$\theta = \theta_o + \theta_1 \frac{r}{R}$$

In general, there would be a segment of the blade/hub which is inboard of the blade pitch bearing and does not rotate with pitch. It is considered that this segment of the blade/hub system extends from the hub to a radius r_h and the stiffness characteristics of this segment are denoted by the subscript h. The outboard segment rotates with pitch and is denoted by the subscript b. In this case, therefore the stiffness coefficients are

$$K^{vv\theta} = \int_o^{r_h} EI_{z'_h} (\psi_v'')^2 \, dr + \int_{r_h}^{R} (EI_{z'_b} \cos^2\theta + EI_{y'_b} \sin^2\theta)(\psi_v'')^2 \, dr$$

$$K^{ww\theta} = \int_o^{r_h} EI_{y'_h} (\psi_w'')^2 \, dr + \int_{r_h}^{R} (EI_{z'_b} \sin^2\theta + EI_{y'_b} \cos^2\theta)(\psi_w'')^2 \, dr$$

$$K^{vw\theta} = \int_{r_h}^{R} (EI_{z'_b} - EI_{y'_b}) \frac{\sin 2\theta}{2} (\psi_v'' \psi_w'') \, dr$$

AERODYNAMIC

$$A^{x\theta v} = \int_o^R r\theta \, \psi_v \, dr$$

$$A^{v} = \int_o^R \psi_v \, dr$$

$$A^{xxv} = \int_o^R r^2 \psi_v \, dr$$

$$A^{xx\theta w} = \int_o^R r^2 \theta \, \psi_w \, dr$$

$$A^{xw} = \int_o^R r \, \psi_w \, dr$$

$$A^{x\theta wv} = \int_o^R r \, \theta \, \psi_w \, \psi_v \, dr = A^{x\theta vw}$$

$$A^{\dot{w}v} = \int_o^R \psi_w \psi_v \, dr = A^{vw}$$

$$A^{\theta vv} = \int_o^R \theta \, \psi_v^2 \, dr$$

$$A^{xwv} = \int_o^R r \, \psi_w \psi_v \, dr$$

If the same mode shapes are used for flap and lag deflections ($\psi_v = \psi_w = \psi$) the following relationships hold among the coefficients:

$$M^{vv} = M^{ww} = -\Omega^2 \, M^{\dot{v}v} = -\Omega^2 \, M^{\dot{w}w}$$

$$K^{V\dot{v}v} = K^{V\dot{v}w} = - M^{uv\dot{v}v} = - M^{uw\dot{w}v}$$

$$K^{Vv} = K^{Vw}$$

$$M^{\dot{v}w} = M^{\dot{w}v} = 2\Omega \beta_{pc} \, M^{\dot{v}v}$$

Define, noting that $(\bar{\ })'$ indicates a derivative with respect to x:

$$\tilde{M}(x_1) = \int_o^{x_1} \psi^2 \, dx$$

$$\tilde{M}^{xw}(x_1) = \int_o^{x_1} x \, \psi \, dx$$

$$\tilde{M}^{uv\dot{v}v}(x_1) = - 2 \int_o^{x_1} c^{uv\dot{v}} \, \psi \, dx$$

$$c^{uv\dot{v}}(x_1) = - \int_o^x (\bar{\psi}')^2 \, d\eta$$

$$\tilde{K} = \int_o^{x_1} (\bar{\psi}'')^2 \, dx$$

$$\tilde{K}^x = \int_o^{x_1} x \, (\bar{\psi}'')^2 \, dx$$

$$\tilde{K}^p(x_1) = \int_o^{x_1} (\bar{\psi}')^2 \, dx$$

$$\tilde{K}^{pxx}(x_1) = \int_o^{x_1} x^2 \, (\bar{\psi}')^2 \, dx$$

If a segmented blade is considered with constant properties within each segment the several coefficients may be expressed more explicitly as given below.

$m^{(1)}$ = running mass of segment located between 0 and x_1.

$m^{(2)}$ = running mass of segment located between x_1 and x_2.

$EI^{(1)}$ = stiffness of segment located between 0 and x_1.

$EI^{(2)}$ = stiffness of segment located between x_1 and x_2.

$\theta_o^{(1)}$ = pitch of segment located between 0 and x_1.

$\theta_o^{(2)}$ = pitch of segment located between x_1 and x_2.

θ_1 = linear twist

The tip of the blade is located at $x_N = 1$.

$$M^{\ddot{V}v} = m^{(1)} \tilde{M}(x_1) + m^{(2)} [\tilde{M}(x_2) - \tilde{M}(x_1)] + \ldots + m^{(N)} [\tilde{M}(x_N) - \tilde{M}(x_{N-1})]$$

$$M^{XW} = \beta_{pc} \Omega^2 R^2 \left\{ m^{(1)} \tilde{M}^{XW}(x_1) + m^{(2)} [\tilde{M}^{XW}(x_2) - \tilde{M}^{XW}(x_1) + \ldots + m^{(N)} [\tilde{M}^{XW}(x_N) - \tilde{M}^{XW}(x_{N-1})] \right\}$$

$$M^{uw\dot{w}v} \equiv M^{uv\dot{v}v} = \Omega \Big\{ m^{(1)} \tilde{M}^{uv\dot{v}v}(x_1) + m^{(2)} [\tilde{M}^{uv\dot{v}v}(x_2) - \tilde{M}^{uv\dot{v}v}(x_1)] + \ldots + m^{(N)} [\tilde{M}^{uv\dot{v}v}(x_N) - \tilde{M}^{uv\dot{v}v}(x_{N-1})] \Big\}$$

STIFFNESS COEFFICIENTS

$$K^{vv\theta} = \frac{EI_{z'}^{(1)}}{R^3} \Big\{ \cos^2 \theta_o^{(1)} \tilde{K}(x_1) - [\sin 2\theta_o^{(1)}] \theta_1 \tilde{K}^x(x_1) \Big\} + \frac{EI_{y'}^{(1)}}{R^3} \Big\{ \sin^2 \theta_o^{(1)} \tilde{K}(x_1) + [\sin 2\theta_o^{(1)}] \theta_1 \tilde{K}(x_1) \Big\} + \ldots + \frac{EI_{z'}^{(N)}}{R^3} \Big\{ \cos^2 \theta_o^{(N)} [\tilde{K}(x_N) - \tilde{K}(x_{N-1})] - [\sin 2\theta_o^{(N)}] \theta_1 [\tilde{K}^x(x_N) - \tilde{K}^x(x_{N-1})] \Big\} + \frac{EI_{y'}^{(1)}}{R^3} \Big\{ \sin^2 \theta_o^{(N)} [\tilde{K}(x_N) - \tilde{K}(x_{N-1})] + [\sin 2\theta_o^{(N)}] \theta_1 [\tilde{K}^x(x_N) - \tilde{K}^x(x_{N-1})] \Big\}$$

$$K^{ww\theta} = \frac{EI_{z'}^{(1)}}{R^3} \Big\{ \sin^2 \theta_o^{(1)} \tilde{K}(x_1) + [\sin 2\theta_o^{(1)}] \theta_1 \tilde{K}^x(x_1) \Big\} + \frac{EI_{y'}^{(1)}}{R^3} \Big\{ \cos^2 \theta_o^{(1)} \tilde{K}(x_1) - [\sin 2\theta_o^{(1)}] \theta_1 \tilde{K}^x(x_1) \Big\} + \ldots$$

$$K^{vw\theta} = K^{wv\theta}$$

$$= \frac{[EI_{z'}^{(1)} - EI_{y'}^{(1)}]}{2R^3} \left(\sin 2\theta_o^{(1)} \tilde{K}(x_1) + 2\theta_1 \cos 2\theta_o^{(1)} \tilde{K}^x(x_1) \right)$$

$$+ \ldots$$

$$K^{Vv} = \Omega^2 R \left\{ \left[m^{(N)} \frac{[x_N^2 - x_{N-1}^2]}{2} + m^{(N-1)} \frac{[x_{N-1}^2 - x_{N-2}^2]}{2} \right.\right.$$

$$\left. + \ldots + \frac{m^{(1)} x_1^2}{2} \right] \tilde{K}^D(x_1)$$

$$- \frac{m^{(1)}}{2} \tilde{K}^{Dxx}(x_1)$$

$$+ \left[m^{(N)} \frac{[x_N^2 - x_{N-1}^2]}{2} + \ldots \right.$$

$$\left. - \frac{m^{(2)}}{2} \right] \left[\tilde{K}^{Dxx}(x_2) - \tilde{K}^{Dxx}(x_1) \right]$$

$$+ \{ \ldots \} \{ \ldots \}$$

$$\{ \ldots \}$$

$$+ \frac{m^{(N)}}{2} x_N^2 \left[\tilde{K}^D(x_N) - \tilde{K}^D(x_{N-1}) \right]$$

$$\left. - \frac{m^{(N)}}{2} \left[\tilde{K}^{Dxx}(x_N) - \tilde{K}^{Dxx}(x_{N-1}) \right] \right\}$$

The various functions of mode shape are shown graphically in Figures A-1 through A-7 for a Duncan Polynomial mode shape

$$\psi = 2x^2 - \frac{4}{3} x^3 + \frac{1}{3} x^4$$

The aerodynamic terms are as follows for this mode shape.

AERODYNAMIC COEFFICIENTS

$$A^{v} = .4R$$

$$A^{xw} = .289R^2$$

$$A^{xxv} = .225R^3$$

$$A^{wv} = .256R$$

$$A^{xwv} = .206R^2$$

$$A^{\theta vv} = .206R\,\theta_1 + .256\,R\,\theta_o$$

$$A^{x\theta wv} = .172R^2\,\theta_1 + .206\,R^2\,\theta_o$$

$$A^{x\theta v} = .225R^2\,\theta_1 + .289R^2\,\theta_o$$

$$A^{xx\theta w} = .185R^3\,\theta_1 + .225R^3\,\theta_o$$

The blade has a constant pitch θ_o and a linear twist represented by θ_1. To place these flexible blade equations in a form which can be conveniently compared to the rigid blade equations, the displacements are nondimensionalized by the rotor radius and each of the equations is multiplied by $(\frac{R}{I_1 \Omega^2})$ where I_1 is the flapping moment of inertia of the blade, $I_1 = \int_o^R mr^2\ dr$. The time is nondimensionalized by the rotor RPM, Ω, such that

$$\bar{v}^o = \frac{v^o}{R}, \quad \bar{w}^o = \frac{w^o}{R}$$

$$\dot{\bar{v}} = \frac{\dot{v}}{\Omega R}, \quad \dot{\bar{w}} = \frac{\dot{w}}{\Omega R}$$

$$\ddot{\bar{v}} = \frac{\ddot{v}}{\Omega^2 R}, \quad \ddot{\bar{w}} = \frac{\ddot{w}}{\Omega^2 R}$$

The equations become, where the primes indicate derivatives of the mode shapes with respect to the dimensionless distance x,

$$\dot{\bar{v}}^{o}\left[\left(\frac{R^2 M^{vv}}{I_1 \Omega^2}\right)+\left(\frac{R^2 K^{Vv}}{I_1 \Omega^2}\right)+\left(\frac{R^2 K^{vv\theta}}{I_1 \Omega^2}\right)\right] + \bar{w}^{o}\left(\frac{R^2 K^{vw\theta}}{I_1 \Omega^2}\right) = \frac{\gamma}{8}\left(\frac{8Q^{y^{o}}}{\rho ac\, R^3 \Omega^2}\right)$$

$$\left(\frac{RM^{xw}}{I_1 \Omega^2}\right) + \bar{w}^{o}\left(\frac{R^2 K^{Vw}}{I_1 \Omega^2} + \frac{R^2 K^{ww\theta}}{I_1 \Omega^2}\right) + \dot{\bar{v}}^{o}\left(\frac{R^2 K^{vw\theta}}{I_1 \Omega^2}\right) = \frac{\gamma}{8}\left(\frac{8Q^{z^{o}}}{\rho ac\, R^3 \Omega^2}\right)$$

$$\dot{\bar{v}}\left(\frac{R^3 M^{uv\dot{v}v}}{I_1 \Omega} + \frac{R^3 K^{V\dot{v}v}}{I_1 \Omega}\right) \bar{v}^{o} + \bar{w}^{o}\left(\frac{R^3 M^{uw\dot{w}v}}{I_1 \Omega} \bar{w}^{o} + \frac{R^2 M^{\dot{w}v}}{I_1 \Omega}\right)$$
$$+ \bar{v}\left(\frac{R^2 M^{vv}}{I_1 \Omega^2} + \frac{R^2 K^{Vv}}{I_1 \Omega^2} + \frac{R^2 K^{vv\theta}}{I_1 \Omega^2}\right) + \bar{w}\left(\frac{R^2 K^{vw\theta}}{I_1 \Omega^2}\right)$$
$$+ \ddot{\bar{v}}\left(\frac{R^2 M^{\ddot{V}v}}{I_1}\right) = \frac{\gamma}{8}\left(\frac{8Q^{y}}{\rho ac\, R^3 \Omega^2}\right)$$

$$\dot{\bar{v}}\left[\left(\frac{R^2 M^{\dot{V}w}}{I_1 \Omega}\right)+\left(\frac{R^3 K^{V\dot{v}w}}{I_1 \Omega}\right)\bar{w}^{o}\right]+\left[\left(\frac{R^2 K^{Vw}}{I_1 \Omega^2}\right)+\left(\frac{R^2 K^{ww\theta}}{I_1 \Omega^2}\right)\right]\bar{w}$$
$$+ \bar{v}\left(\frac{R^2 K^{vw\theta}}{I_1 \Omega^2}\right)+\ddot{\bar{w}}\left(\frac{R^2 M^{\dot{w}w}}{I_1}\right) = \frac{\gamma}{8}\left(\frac{8Q^{z}}{\rho ac\, R^3 \Omega^2}\right)$$

The dimensionless terms appearing in the above equations are denoted by small letters and $\bar{m} = mR$

$$m^{vv} = \frac{R^2 M^{vv}}{I_1 \Omega^2} = \frac{-\int_o^1 \bar{m}\, \psi_v^2\, dx}{\int_o^1 \bar{m}\, x^2\, dx}$$

$$m^{\ddot{v}v} = \frac{R^2 M^{\ddot{v}v}}{I_1} = \frac{-\int_o^1 \bar{m}\,\psi_v^2\,dx}{\int_o^1 \bar{m}x^2\,dx} = -m^{vv}$$

$$m^{\ddot{w}w} = \frac{R^2 M^{\ddot{w}w}}{I_1} = \frac{\int_o^1 \bar{m}\,\psi_w^2\,dx}{\int \bar{m}\,x^2\,dx} = -m^{ww}$$

$$m^{\dot{v}w} = -m^{\dot{w}v} = \frac{R^2 M^{\dot{v}w}}{I_1\,\Omega} = \frac{2\beta_{pc}\int_o^1 \bar{m}\,\psi_v\,\psi_w\,dx}{\int_o^1 \bar{m}\,x^2\,dx}$$

$$m^{xw} = \frac{R\,M^{xw}}{I_1\,\Omega^2} = \frac{\beta_{pc}\int_o^1 \bar{m}\,x\,\psi_w\,dx}{\int_o^1 \bar{m}\,x^2\,dx}$$

$$m^{uv\dot{v}v} = \frac{R^3 M^{uv\dot{v}v}}{I_1\,\Omega} = \frac{2\int_o^1 \bar{m}\,c^{uv\dot{v}}\,\psi_v\,dx}{\int_o^1 \bar{m}\,x^2\,dx}$$

where

$$c^{uv\dot{v}} = -\int_o^x (\psi_v')^2\,d\eta$$

$$m^{uw\dot{w}v} = \frac{R^3 M^{uw\dot{w}v}}{I_1\,\Omega} = \frac{2\int_o^1 \bar{m}\,c^{uw\dot{w}}\,\psi_w\,dx}{\int \bar{m}\,x^2\,dx}$$

$$k^{V\dot{v}v} = \frac{R^3 K^{V\dot{v}v}}{I_1\,\Omega} = \frac{\int_o^1 c^{m\dot{v}}(\psi_w')^2\,dx}{\int_o^1 \bar{m}\,x^2\,dx}$$

$$c^{m\dot{v}} = 2\int_x^1 \bar{m}\,\psi_v\,d\eta$$

$$k^{V\dot{w}w} = \frac{R^3 K^{V\dot{w}w}}{I^1 \Omega} = \frac{\int_o^1 c^{m\dot{v}} (\psi_w')^2 \, dx}{\int \overline{m} x^2 \, dx}$$

and

$$k^{V\dot{v}v} = -m^{uv\dot{v}v}$$

The aerodynamic terms are, denoting by small a's the dimensionless form of the A's times 4,

$$a^{x\theta v} = \frac{4A^{x\theta v}}{R^2} = 4\int_o^1 x \, \theta \, \psi_v \, dx$$

and $\lambda = -\frac{v_{in}}{\Omega R}$

$$\frac{8Q^{y^o}}{\rho ac R^3 \Omega^2} = -\left[-\lambda \, a^{x\theta v} - \lambda^2 a^v + \frac{C_{do}}{a} a^{xxv}\right]$$

$$\frac{8Q^{z^o}}{\rho ac R^3 \Omega^2} = -\left[-a^{xx\theta w} - \lambda \, a^{xw}\right]$$

$$\frac{8Q^y}{\rho ac R^3 \Omega^2} = -\left[\dot{\overline{w}} \left(a^{x\theta wv} + 2\lambda \, a^{wv}\right) + \dot{\overline{v}} \left(-\lambda \, a^{\theta vv} + 2\frac{C_{do}}{a} a^{xwv}\right)\right]$$

$$\frac{8Q^z}{\rho ac R^3 \Omega^2} = -\left[\dot{\overline{w}} \, a^{xwv} + \dot{\overline{v}} \left(-\lambda \, a^{vw} - 2 \, a^{x\theta vw}\right)\right]$$

The stiffness terms are

$$k^{Vv} = \frac{R^2 K^{Vv}}{I_1 \Omega^2} = \frac{\int_o^1 C^{mx} (\psi_v')^2 \, dx}{\int \overline{m} x^2 \, dx}$$

$$k^{Vw} = \frac{R^2 K^{Vw}}{I_1 \Omega^2} = \frac{\int_o^1 c^{mx} (\psi_w')^2 \, dx}{\int \overline{m} x^2 \, dx}$$

$$c^{mx} = \int_x^1 \bar{m}\,\eta\,d\eta$$

$$k^{vv\theta} = \frac{R^2 K^{vv\theta}}{I_1 \Omega^2} = \frac{1}{R^3 \Omega^2} \frac{\int_o^1 (EI_z' \cos^2\theta + EI_y' \sin^2\theta)(\psi_v'')^2\,dx}{\int_o^1 \bar{m}\,x^2\,dx}$$

$$k^{ww\theta} = \frac{R^2 K^{ww\theta}}{I_1 \Omega^2} = \frac{1}{R^3 \Omega^2} \frac{\int_o^1 (EI_z' \sin^2\theta + EI_y' \cos^2\theta)(\psi_w'')^2\,dx}{\int_o^1 \bar{m}\,x^2\,dx}$$

$$k^{vw\theta} = \frac{R^2 K^{vw\theta}}{I^1 \Omega^2} = \frac{1}{R^3 \Omega^2} \frac{\int_o^1 (EI_z' - EI_y') \frac{\sin 2\theta}{2} (\psi_v'' \psi_w'')\,dx}{\int_o^1 \bar{m}\,x^2\,dx}$$

The equations become, using this notation,

Steady State Equations

$$(m^{vv} + k^{Vv} + k^{vv\theta})\,\bar{v}^o + k^{vw\theta}\,\bar{w}^o = \frac{\gamma}{8}\left(\lambda\, a^{x\theta v} + \lambda^2 a^{v} - \frac{C_{do}}{a} a^{xxv}\right)$$

$$m^{xw} + (k^{Vw} + k^{ww\theta})\,\bar{w}^o + k^{vw\theta}\,\bar{v}^o = \frac{\gamma}{8}\left(a^{xx\theta w} + \lambda\, a^{xw}\right)$$

Perturbation Equations

$$\dot{\bar{w}}\,(m^{uw\dot{w}v}\,\bar{w}^o + m^{\dot{w}v}) + \bar{v}\,(m^{vv} + k^{Vv} + k^{vv\theta})$$

$$+ \bar{w}\,k^{vw\theta} + \ddot{\bar{v}}\,m^{\ddot{v}v} = \frac{\gamma}{8}\left(-\dot{w}\,(a^{x\theta wv} + 2\lambda\, a^{wv}) + \dot{\bar{v}}\,(+\lambda\, a^{\theta vv} - 2\frac{C_{do}}{a} a^{xwv})\right)$$

$$\dot{\bar{v}}\,(m^{\dot{v}w} + k^{V\dot{v}w}\,\bar{w}^o) + \bar{w}\,(k^{Vw} + k^{ww\theta}) + \bar{v}\,(k^{vw\theta})$$

$$+ \ddot{\bar{w}}\,m^{\ddot{w}w} = \frac{\gamma}{8}\left(-\dot{\bar{w}}\,a^{xwv} + \dot{\bar{v}}\,(+\lambda\, a^{vw} + 2\, a^{x\theta vw})\right)$$

Dividing the perturbation equations by the coefficients of the acceleration terms and collecting terms on the left hand side.

$$\ddot{\bar{v}} + \frac{\gamma}{8}\left(2\,\frac{C_{do}}{a}\,\left(\frac{a^{xwv}}{m^{\dot{v}v}}\right) - \lambda\,\left(\frac{a^{\theta vv}}{m^{\dot{v}v}}\right)\right)\dot{\bar{v}} + \left(\frac{m^{vv} + k^{Vv} + k^{vv\theta}}{m^{\dot{v}v}}\right)\bar{v}$$

$$+ \dot{\bar{w}}\left(\frac{m^{uw\dot{w}v}}{m^{\dot{v}v}}\,\bar{w}^{o} + \frac{m^{\dot{w}v}}{m^{\dot{v}v}} + \frac{\gamma}{8}\left(\frac{a^{x\theta wv}}{m^{\dot{v}v}} + 2\lambda\,\frac{a^{wv}}{m^{\dot{v}v}}\right)\right) + \bar{w}\,\left(\frac{k^{vw\theta}}{m^{\dot{v}v}}\right) = 0$$

$$\ddot{\bar{w}} + \frac{\gamma}{8}\,\left(\frac{a^{xwv}}{m^{\dot{w}w}}\right)\dot{\bar{w}} + \left(\frac{k^{Vw} + k^{ww\theta}}{m^{\dot{w}w}}\right)\bar{w} + \dot{\bar{v}}\left(\frac{m^{\dot{v}w}}{m^{\dot{w}w}} + \left(\frac{k^{V\dot{v}w}}{m^{\dot{w}w}}\right)\bar{w}^{o}\right.$$

$$\left. - \frac{\gamma}{8}\,\left(\lambda\,\frac{a^{vw}}{m^{\dot{w}w}} + 2\,\frac{a^{x\theta vw}}{m^{\dot{w}w}}\right)\right) + \bar{v}\,\left(\frac{k^{vw\theta}}{m^{\dot{w}w}}\right) = 0$$

For zero precone,

$$m^{\dot{w}v} = 0$$

$$m^{\dot{v}w} = 0$$

and defining the dimensionless uncoupled frequencies as,

$$p^2 = \frac{k^{Vw} + k^{ww\theta}}{m^{\dot{w}w}}$$

$$q^2 = \frac{m^{vv} + k^{Vv} + k^{vv\theta}}{m^{\dot{v}v}}$$

the coefficients of the Coriolis terms as,

$$C_o^{vv} = \frac{m^{uw\dot{w}v}}{m^{\dot{v}v}}$$

$$C_o^{ww} = \frac{k^{V\dot{v}w}}{m^{\dot{w}w}}$$

and the elastic coupling terms as

$$C_1^{vv} = \frac{k^{vw\theta}}{\ddot{m}^{vv}}$$

$$C_1^{ww} = \frac{k^{vw\theta}}{\ddot{m}^{ww}}$$

the equations are

$$\ddot{\bar{v}} + \frac{\gamma}{8}\left(2\frac{C_{do}}{a}\left(\frac{a^{xwv}}{\ddot{m}^{vv}}\right) - \lambda\frac{a^{\theta vv}}{\ddot{m}^{vv}}\right)\dot{\bar{v}} + q^2\bar{v}$$

$$+ \dot{\bar{w}}\left(C_o^{vv}\bar{w}^o + \frac{\gamma}{8}\left(\frac{a^{x\theta wv}}{\ddot{m}^{vv}} + 2\lambda\frac{a^{wv}}{\ddot{m}^{vv}}\right)\right) + C_1^{vv}\,w = 0$$

$$\ddot{\bar{w}} + \frac{\gamma}{8}\left(\frac{a^{xwv}}{\ddot{m}^{ww}}\right)\dot{\bar{w}} + p^2\bar{w} + \dot{\bar{v}}\left(C_o^{ww}\bar{w}^o - \frac{\gamma}{8}\left(\lambda\frac{a^{vw}}{\ddot{m}^{ww}} + 2\frac{a^{x\theta vw}}{\ddot{m}^{ww}}\right)\right) + C_1^{ww}\bar{v} = 0$$

If the mode shapes are assumed to be the same for both deflections then,

$$\ddot{m}^{ww} = \ddot{m}^{vv}$$

$$C_o = -C_o^{vv} = C_o^{ww}$$

$$C_1 = C_1^{vv} = C_2^{ww}$$

and defining

$$\tilde{a}^{ii} = \frac{a^{ii}}{\ddot{m}^{vv}} = \frac{a^{ii}}{\ddot{m}^{ww}}$$

the equations are, recalling that λ is the inflow angle at the blade tip,

$$\ddot{\bar{v}} + \frac{\gamma}{8}\left(2\frac{C_{do}}{a}\tilde{a}^{xwv} - \lambda\,\tilde{a}^{\theta vv}\right)\dot{\bar{v}} + q^2\bar{v}$$

$$+ \dot{\bar{w}}\left(-C_o\bar{w}^o + \frac{\gamma}{8}\left(\tilde{a}^{x\theta wv} + 2\lambda\,\tilde{a}^{wv}\right)\right) + C_1\bar{w} = 0$$

$$\ddot{\bar{w}} + \frac{\gamma}{8} \tilde{a}^{xwv} \dot{\bar{w}} + p^2 \bar{w} + \dot{\bar{v}} \left(C_o \bar{w}^o - \frac{\gamma}{8} (\lambda \tilde{a}^{vw} + 2 \tilde{a}^{x\theta vw}) \right) + C_1 \bar{v} = 0$$

Now these equations are in a form which may be compared with the rigid blade equations. If a rigid blade model is employed, then the spring constants for the rigid blade model are identified in such a way that the parallel spring model gives identical coefficients to the stiffness terms represented by p^2, q^2 and C_1 as well as in the calculation of the coning angle $\bar{w}_o$. The significance of these changes is considered elsewhere in this report.

The steady state equations are

$$q^2 \bar{v}^o + C_1 \bar{w}^o = \frac{\gamma}{8} \left(\lambda \tilde{a}^{x\theta v} + \lambda^2 \tilde{a}^{v} - \frac{C_{do}}{a} \tilde{a}^{xxv} \right)$$

$$p^2 \bar{w}^o + C_1 \bar{v}^o = \frac{\gamma}{8} \left(\tilde{a}^{xx\theta w} + \lambda \tilde{a}^{xw} \right)$$

The rigid blade terms can be obtained by substitution of $\psi = x$ in the expressions given above.

TABLE I

COMPARISON OF
COEFFICIENTS IN FLAP-LAG EQUATIONS FOR RIGID BLADE
AND DUNCAN POLYNOMIAL MODE SHAPE. UNIFORM MASS DISTRIBUTION

Aerodynamic Terms

	$\psi_v = \psi_w = x$	$\psi_v = \psi_w = 2x^2 - \frac{4}{3}x^3 + \frac{1}{3}x^4$
$a^{x\theta v}$	$1.333\,\theta_o + \theta_1$	$1.156\,\theta_o + .900\,\theta_1$
a^{v}	2.00	1.600
a^{xxv}	1.00	.900
$a^{xx\theta w}$	$1.00\,\theta_o + .800\,\theta_1$	$.900\,\theta_o + .738\,\theta_1$
a^{xw}	1.333	1.156
$a^{x\theta wv}$	$1.00\,\theta_o + .800\,\theta_1$	$.824\,\theta_o + .687\,\theta_1$
$a^{vw} = a^{wv}$	1.333	1.028
$a^{\theta vv}$	$1.333\,\theta_o + 1.00\,\theta_1$	$1.028\,\theta_o + .824\,\theta_1$
a^{xwv}	1.000	.824

Mass Terms (uniform mass blade)

	$\psi_v = \psi_w = x$	$\psi_v = \psi_w = 2x^2 - \frac{4}{3}x^3 + \frac{1}{3}x^4$
m^{vv}	- 1	- .770
$m^{\ddot{v}v}$	1	.770
$m^{\dot{v}w}$	$2\beta_{pc}$	$1.542\,\beta_{pc}$
m^{xw}	β_{pc}	$.867\,\beta_{pc}$
$-m^{uw\dot{w}v}$	2	1.625

Stiffness (uniform stiffness blade)

	$\psi_v = \psi_w = x$	$\psi_v = \psi_w = 2x^2 - \frac{4}{3}x^3 + \frac{1}{3}x^4$
$k^{V\dot{v}v}$	2	1.625
$k^{V\dot{v}w}$	2	1.625
$k^{Vv} = k^{Vw}$	1	.904

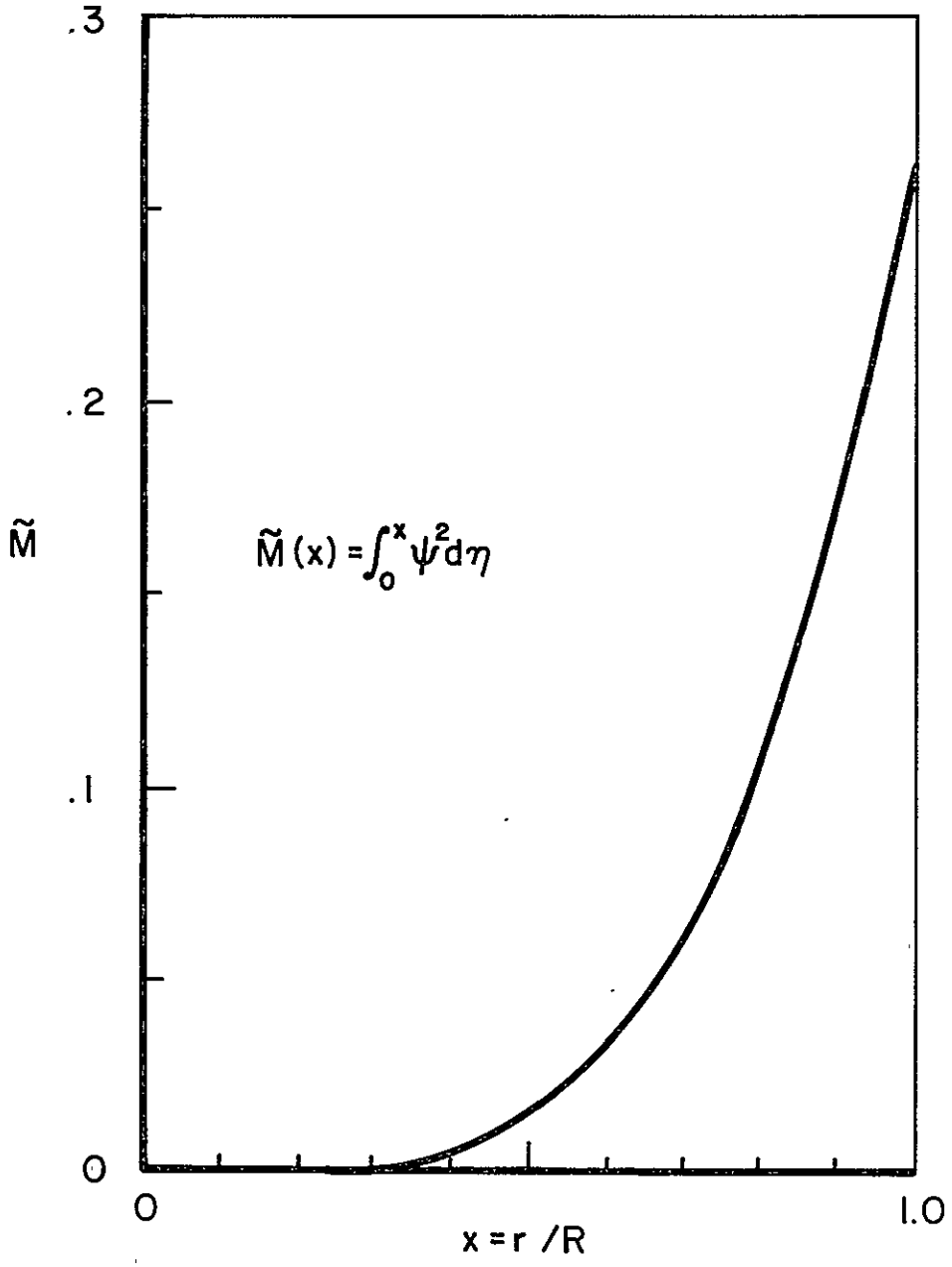

FIGURE A-1. MODE SHAPE INTEGRAL

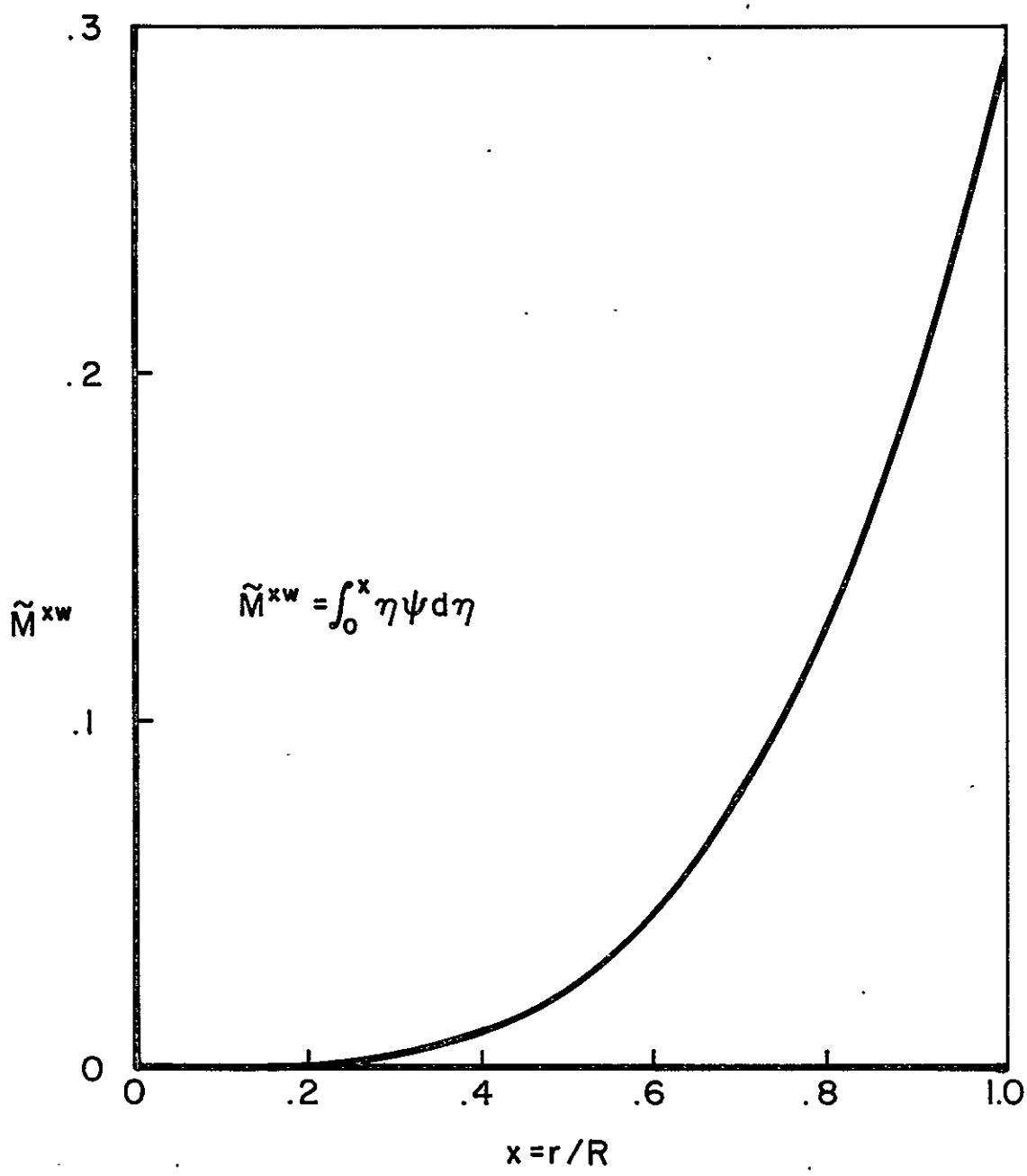

FIGURE A-2. MODE SHAPE INTEGRAL

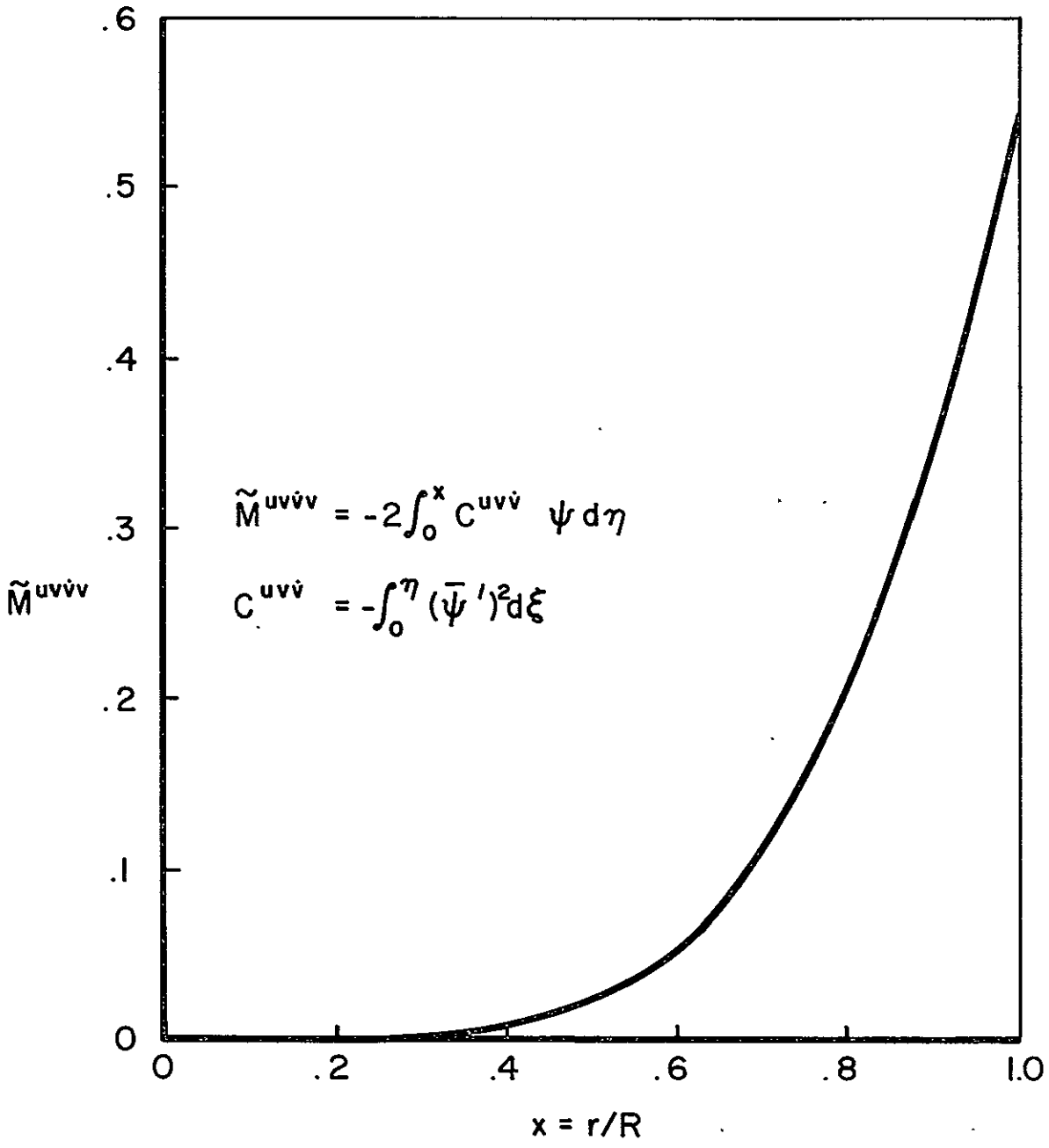

FIGURE A-3. MODE SHAPE INTEGRAL

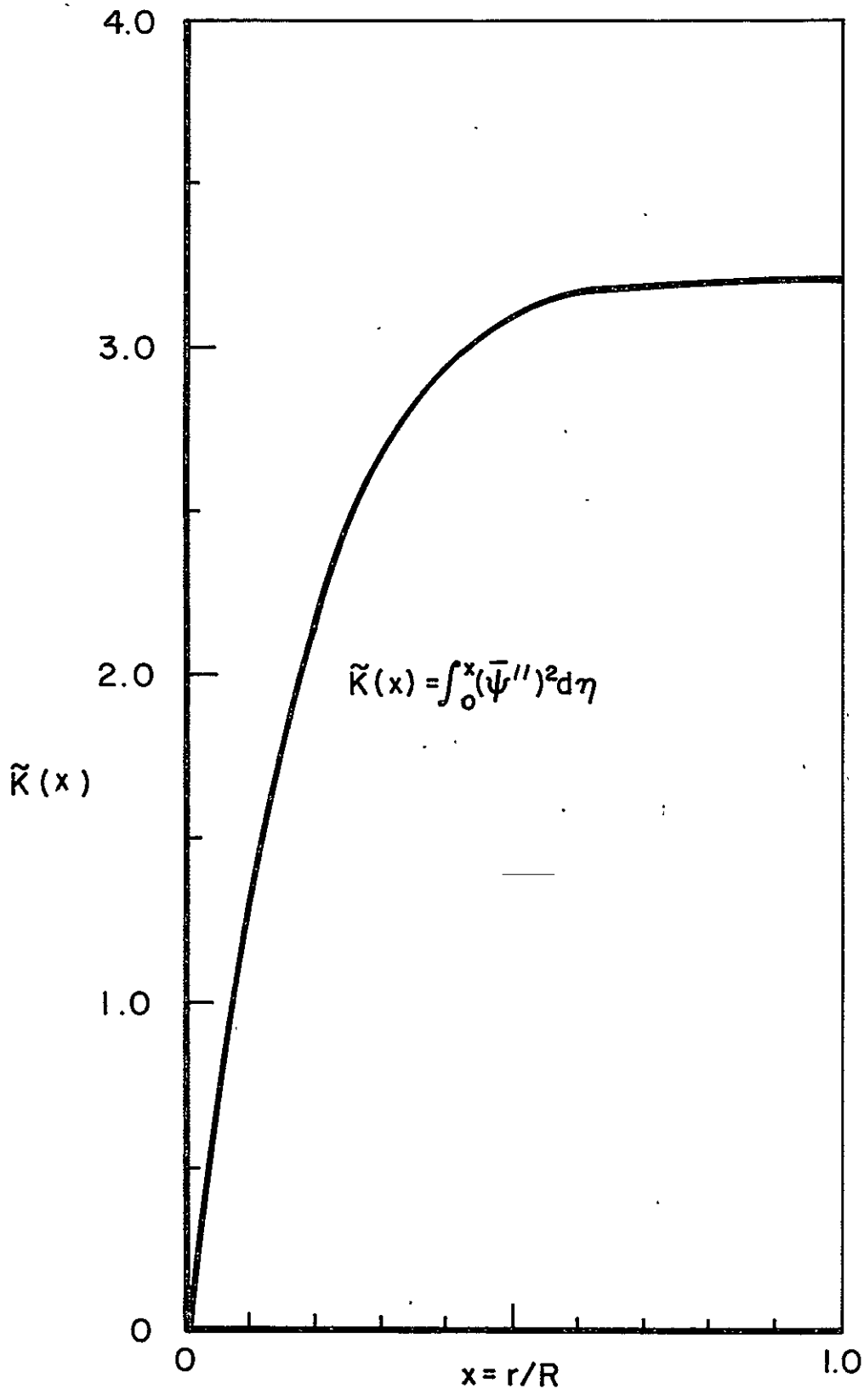

FIGURE A-4. MODE SHAPE INTEGRAL

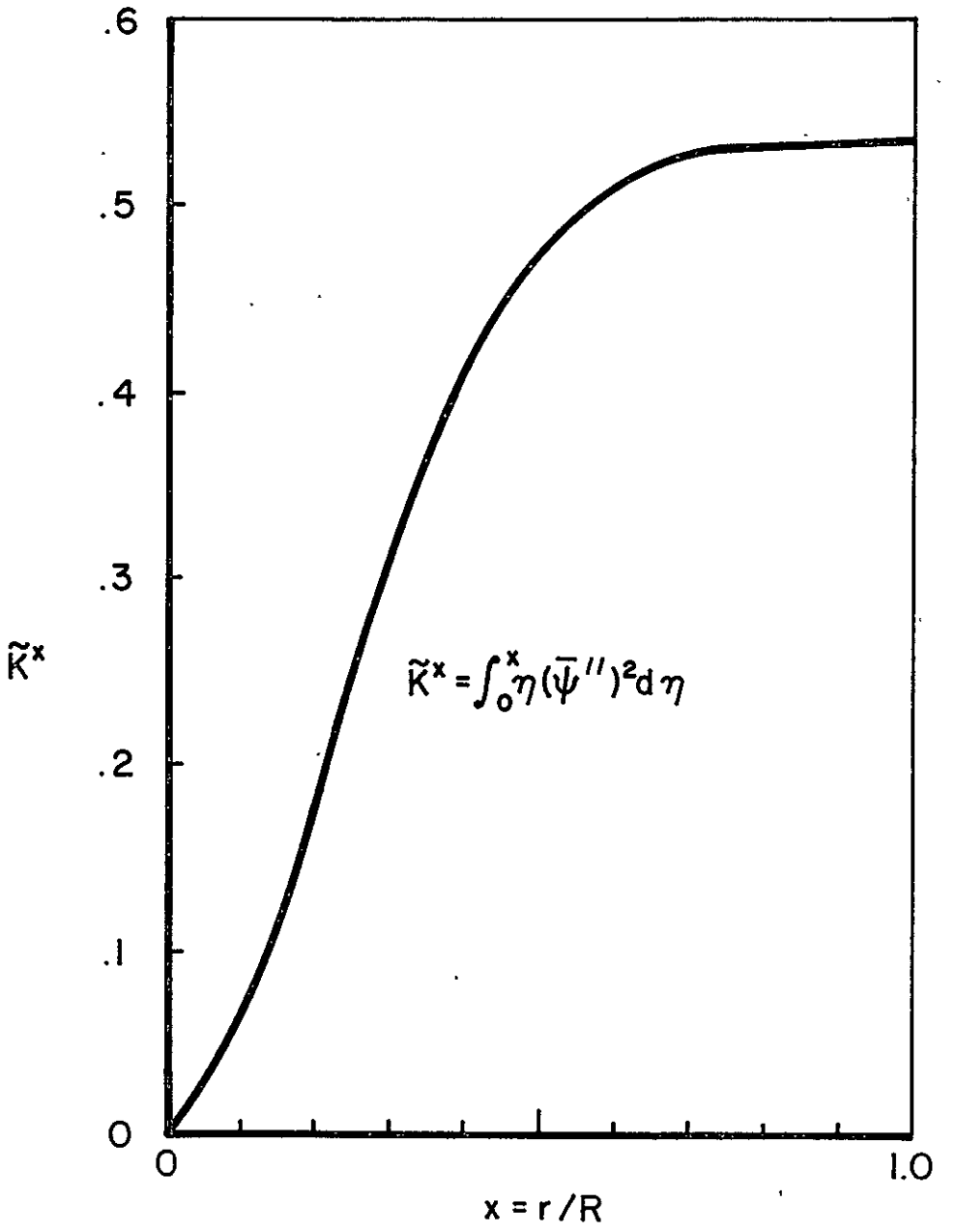

FIGURE A-5. MODE SHAPE INTEGRAL

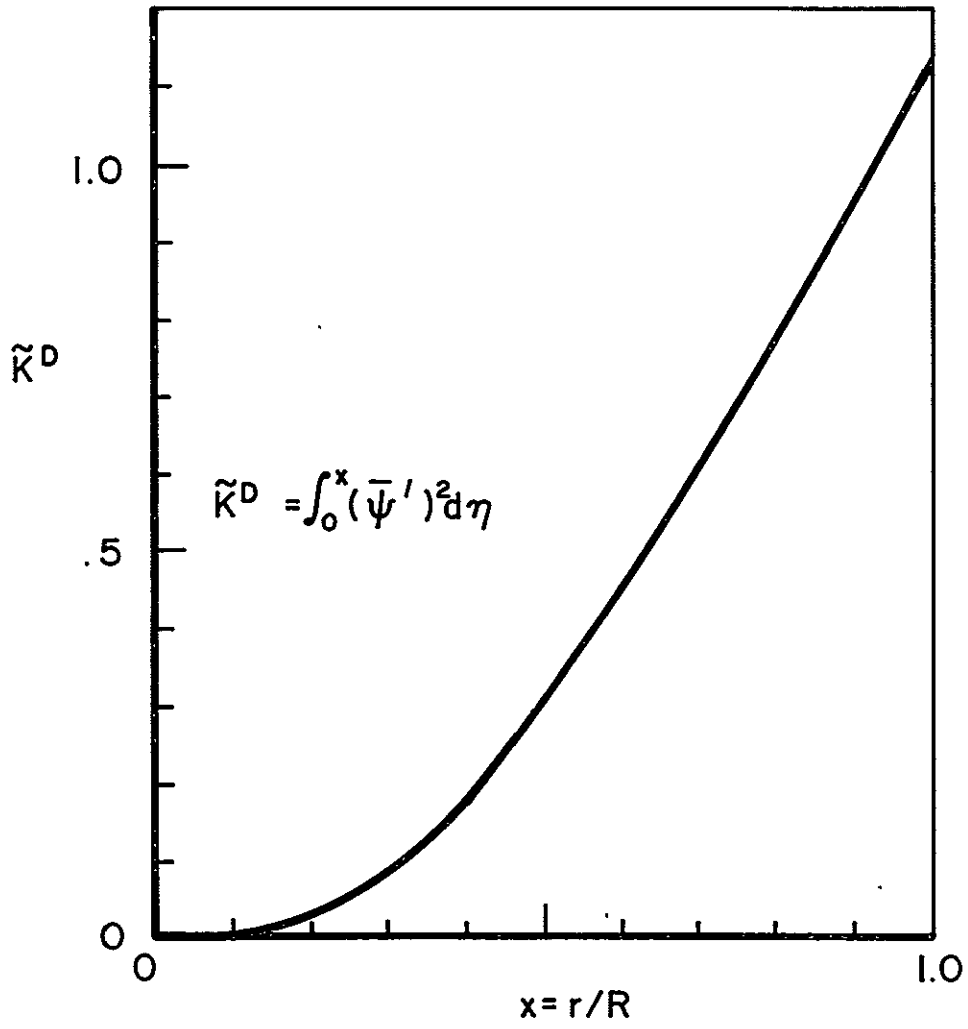

FIGURE A-6. MODE SHAPE INTEGRAL

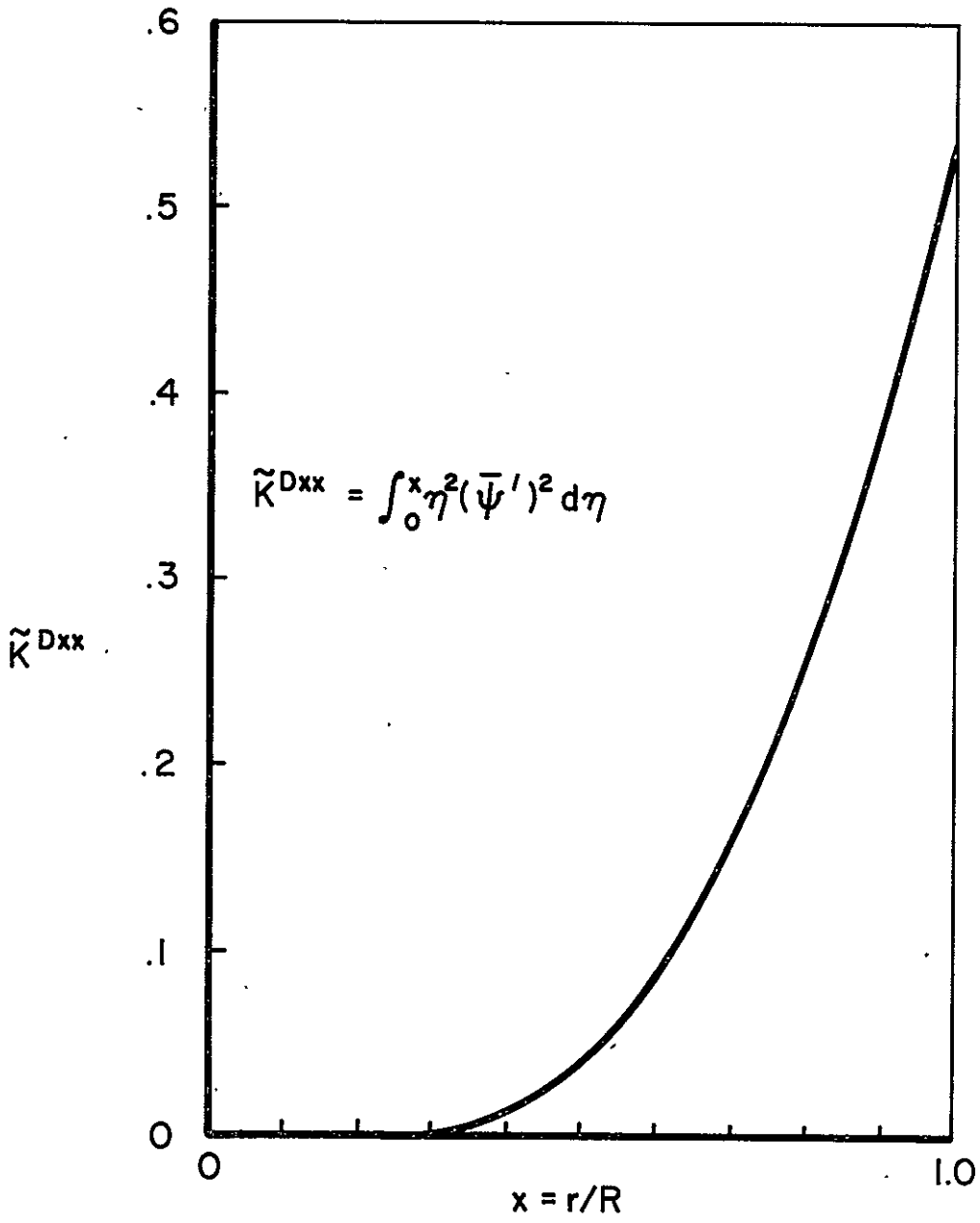

FIGURE A-7. MODE SHAPE INTEGRAL